Geophysical Journal International

Geophys. J. Int. (2011) **184,** 90–110 doi: 10.1111/j.1365-246X.2010.04867.x

Joint geophysical and petrological models for the lithosphere structure of the Antarctic Peninsula continental margin

Tamara Yegorova,[1] Vladimir Bakhmutov,[1] Tomasz Janik[2] and Marek Grad[2,3]

[1] *Institute of Geophysics, National Academy of Sciences of the Ukraine, Palladin av.* 32, 03680 *Kiev, Ukraine. E-mail:egorova@igph.kiev.ua*
[2] *Institute of Geophysics, Polish Academy of Sciences, Ks. Janusza* 64, 01-452 *Warsaw, Poland*
[3] *Institute of Geophysics, Faculty of Physics, University of Warsaw, Pasteura* 7, 02-093 *Warsaw, Poland*

Accepted 2010 October 21. Received 2010 October 10; in original form 2010 March 5

SUMMARY

The Antarctic Peninsula (AP) is a composite magmatic arc terrane formed at the Pacific margin of Gondwana. Through the late Mesozoic and Cenozoic subduction has stopped progressively from southwest to northeast as a result of a series of ridge trench collisions. Subduction may be active today in the northern part of the AP adjacent to the South Shetland Islands. The subduction system is confined by the Shackleton and Hero fracture zones. The magmatic arc of the AP continental margin is marked by high-amplitude gravity and magnetic anomaly belts reaching highest amplitudes in the region of the South Shetland Islands and trench. The sources for these anomalies are highly magnetic and dense batholiths of mafic bulk composition, which were intruded in the Cretaceous, due to partial melting of upper-mantle and lower-crustal rocks. 2-D gravity and magnetic models provide new insights into crustal and upper-mantle structure of the active and passive margin segments of the northern AP. Our models incorporate seismic refraction constraints and physical property data. This enables us to better constrain both Moho geometry and petrological interpretations in the crust and upper mantle. Model along the DSS-12 profile crosses the AP margin near the Anvers Island and shows typical features of a passive continental margin. The second model along the DSS-17 profile extends from the Drake Passage through the South Shetland Trench/Islands system and Bransfield Strait to the AP and indicates an active continental margin linked to slow subduction and on-going continental rifting in the backarc region. Continental rifting beneath the Bransfield Strait is associated with an upward of hot upper mantle rocks and with extensive magmatic underplating.

Key words: Gravity anomalies and earth structure; Magnetic anomalies: modelling and interpretation; Composition of the continental crust; Composition of the oceanic crust; Controlled source seismology; Antarctica.

1 INTRODUCTION

The Antarctic Peninsula (AP) is the most accessible region of West Antarctica for study of the deep structure and tectonic processes which occurred along the southeast Pacific continental margin. The peculiarities of the crustal structure and tectonic processes are manifested in the patterns of geophysical fields. The continental margin here is marked by belts of strong gravity and magnetic anomalies that are generally attributed to a magmatic arc system consisting of a series of plutons and batholiths of assumed different composition and age (Renner *et al.* 1985; Garrett & Storey 1987; Garrett 1990). Recent geophysical data suggest, however a more complex situation. Aerogeophysical survey in Palmer Land, and southern AP, provide support for a composite terrane history of the AP with a major episode of accretion in mid-Cretaceous time (Vaughan & Storey 2000; Ferraccioli *et al.* 2006). Satellite, aero and ship-born potential field data have been compiled into publicly available databases of the ADMAP and ADGRAV projects and are published in many papers (McAdoo & Laxon 1997; Golynsky *et al.* 2001; Kim *et al.* 2002, 2007; Jokat *et al*. 2003; Ferraccioli *et al.* 2006, 2007).

The shelf of AP is the best-studied area in Antarctica by seismic refraction study. During the last thirty years the Polish Academy of Sciences has carried out a refraction seismic study on a network of deep seismic soundings (DSS refraction study) profiles across and along the AP shelf. These investigations allowed the study of crustal and upper mantle structure of the region and the development of a map of depths to the Moho boundary (Grad *et al.* 1992, 2002; Środa *et al.* 1997; Guterch *et al.* 1998; Janik *et al.* 2006; Majdański *et al.* 2008).

Despite great progress having been achieved through studying the deep structure of the AP margin of the Pacific Ocean by a variety of geophysical methods, there is a necessity to carry out a

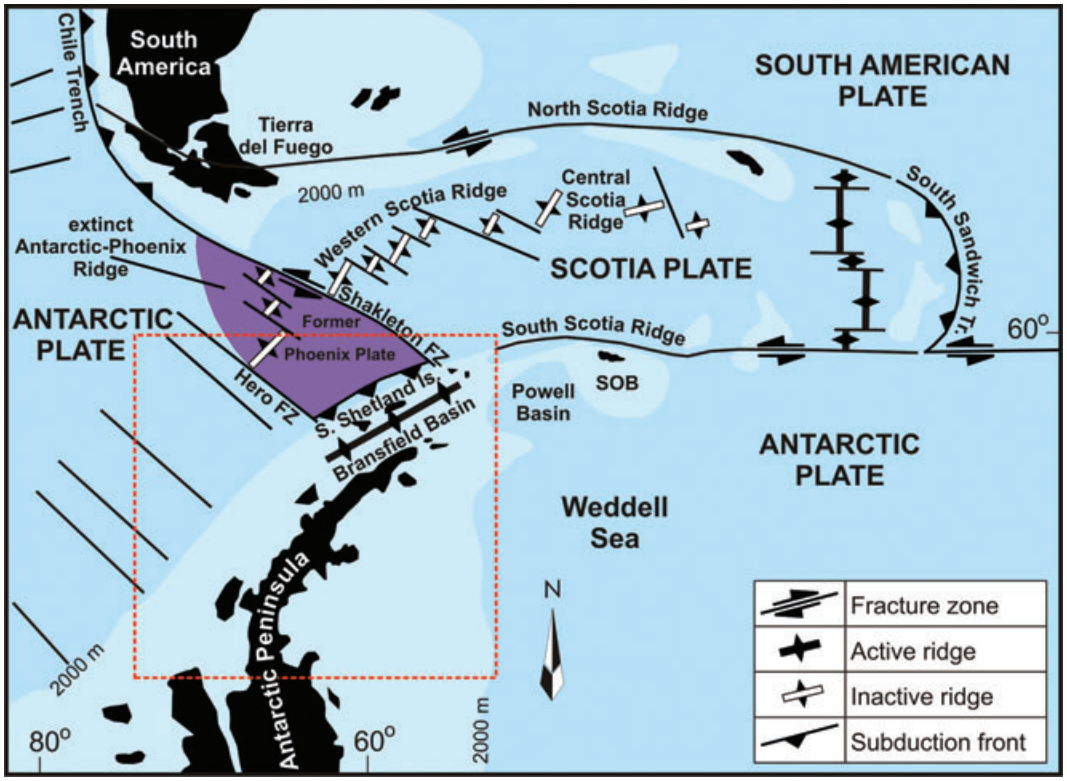

Figure 1. Main tectonic units of Antarctic Peninsula and Scotia Sea (Larter & Barker 1991). Dashed red line rectangle indicates the study area. Light blue shows bathymetry shallower than 2000 m. SOB – South Orkney Block.

joint geophysical interpretation of these data by using models that take into account several geophysical parameters. Thus the main objective of our study is to develop a series of joint geophysical models along the interpretation profiles that cross the continental margin of the AP at the location of the DSS profiles (for location see Figs 1 and 2). As a basis for implementing 2-D gravity and magnetic modelling we used velocity models on the most representative and lengthy seismic profiles within the study region. For the modelling we used satellite-derived Free-Air gravity anomalies (Sandwell & Smith 1997) and total field magnetic anomalies (Golynsky *et al.* 2001). Our joint gravity and magnetic models are further constrained by physical properties of rock samples including the datasets collected during Ukrainian Antarctic expeditions. By combining potential field modelling with seismic refraction and physical property data we delineate the contrasting structure of the lithosphere for the active and passive margin segments of the northern AP.

2 GEOLOGICAL AND TECTONIC SETTING

The AP consists of a number of large domains and is the largest tectonic block of West Antarctica. In contrast to East Antarctica, the main part of which consists of Precambrian rocks, West Antarctica is a geologically complex entity with Phanerozoic rock complexes (Grikurov 1973; Dalziel & Elliot 1982). The AP has been traditionally regarded as a magmatic arc formed along the palaeo-Pacific margin due to Gondwana breakup (Storey & Garret 1985). Recent geophysical and geological studies suggest that the AP is a composite magmatic arc comprising two or three separate terranes that were accreted and sutured along the Gondwana margin in the mid-Cretaceous (Vaughan & Storey 2000; Ferraccioli *et al.* 2006). The two suspect terranes (the Western and Central Domains) have faulted contacts with continental Gondwana margin rocks (Eastern Domain), suggesting that any docking between the former domains and the Gondwana margin was probably dextral-oblique (Vaughan *et al.* 2002).

Recent palaeotectonic reconstructions show that in Late Cretaceous the AP was affected by southeastward subduction of Phoenix Plate, all of which was subducted at the western AP continental margin (Larter *et al.* 2002). Through the late Mesozoic and Cenozoic subduction has stopped progressively from southwest to northeast as a result of a series of ridge trench collisions (Larter & Barker 1988). Subduction is only active today in the northern part of the AP adjacent to the South Shetland Islands located between the Shackleton and Hero fracture zones (Fig. 1). There are three contrasting interpretations for the subduction in the South Shetland Trench: (i) it ceased *ca*. 4 Ma (Barker 1982); (ii) it is on-going, and slow (Pelayo & Wiens 1989; Robertson *et al.* 2003) or (iii) slab-roll back occurred in connection with the cessation of subduction *ca.* 3.3 Ma (Gràcia *et al.* 1996; Galindo-Zaldivar *et al.* 1996, 2004). These processes led to the opening of a backarc basin in the Bransfield Strait (Pelayo & Wiens 1989; Larter & Barker 1991; Galindo-Zaldivar *et al.* 1996, 2004).

Origination of the Bransfield rift is related to the southwestward progradation of tectonic strain associated with stress produced by the South Scotia Ridge (Klepeis & Lawver 1996; González-Casado *et al.* 2000; Jin *et al.* 2002; Fretzdorff *et al.* 2004; Udintsev & Shenke 2004). This corresponds to the general geodynamic setting of the study region (Fig. 1), which defines the evolution of the northern part of the AP as having been affected strongly by microplate dynamics

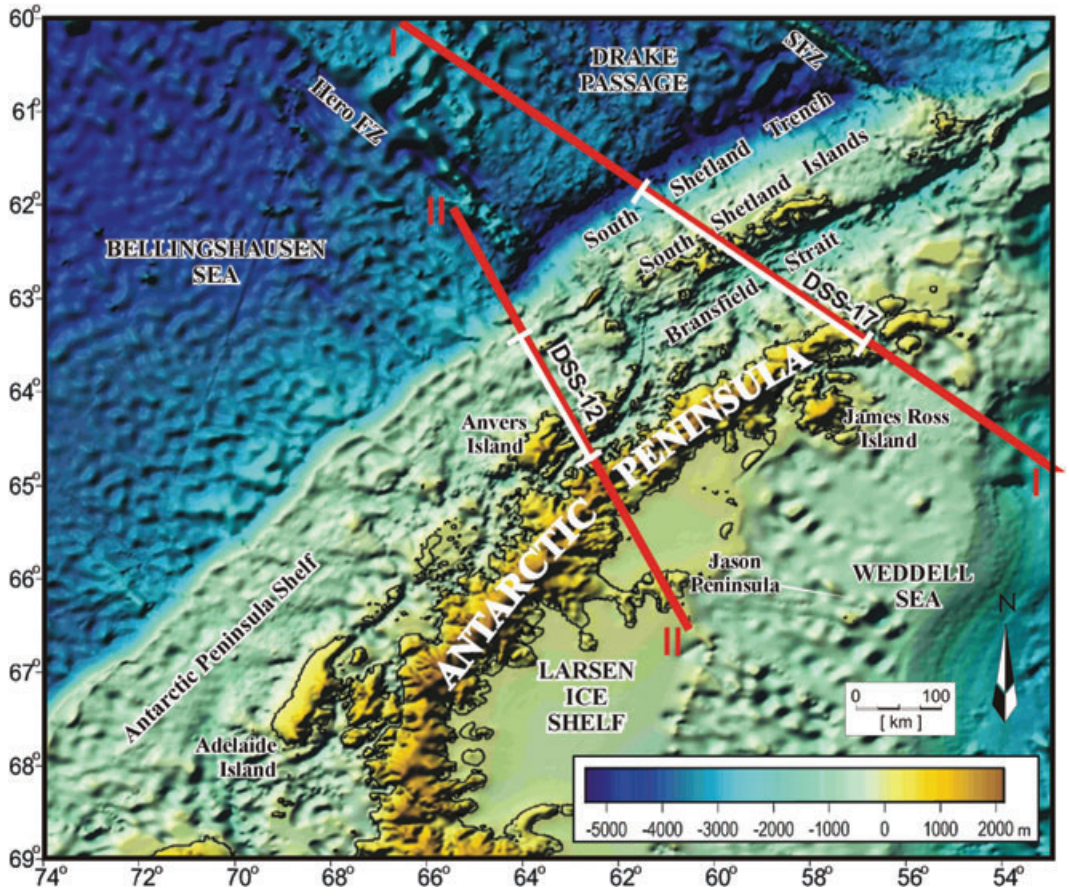

Figure 2. Bathymetry of the study region (Sandwell & Smith 1997) and location of interpretation lines I-I and II-II (red lines) together with selected seismic profiles (white lines) used for 2-D gravity and magnetic modelling.

of the Scotia Arc, in particular by the kinematics and dynamics of the South Scotia Ridge (strike-slip tectonics along the South Scotia Ridge; Pelayo & Wiens 1989). In general, the present-day geodynamics and seismicity of the region of the AP and Scotia Plate are determined by the dynamics and kinematics of the Antarctic Plate (AN), Scotia Plate (SC) and South American Plate (SA). Predicted velocities of westward motion of SA (2.2 cm yr^{-1}) and SC (1.4 cm yr^{-1}) relatively to S–SW slow motion of AN (0.5 cm yr^{-1}) leads to a situation where the North Scotia Ridge shows left-lateral strike-slip motion with a component of convergence, and the South Scotia ridge shows left-lateral motion with a component of extension (Pelayo & Wiens 1989). Convergence between the SC and AN in Drake Passage region appears to be accomodated by diffuse compressional deformation as well as strike-slip faulting along the Shackleton fracture zone (Pelayo & Wiens 1989).

The main seismogenic zones within our study region occur along the South Scotia Ridge and its southwestern extension within the Bransfield Basin, and within the Shackleton fracture zone (Fig. 1). Seismic activity of the South Shetland Trench can be explained by active subduction and backarc spreading along the South Shetland Trench and Bransfield Strait; the maximum depth of seismicity is ∼65 km, but the majority of events are shallower than 30 km (Pelayo & Wiens 1989; Robertson *et al.* 2003).

The main tectonic units in the region of the AP and Scotia Sea are seen in the sea floor bathymetry, which shows the uplifted block of the AP extending eastwards along the South Scotia Ridge as far as the South Orkney block. The AP currently has a clear continental margin along its 2000-km-long boundary with the Pacific. We focus our study on the structure of the Pacific margin of the AP (Fig. 1) in the area of the South Shetland Islands and Bransfield Strait, as well the passive margin section of the AP shelf.

The Bransfield rift is a Late Cenozoic tensional structure, about 40 km wide near King George Island, reaching 100 km width in some places. Measurements of the surface heat flow in the Bransfield Strait show very high values: one quarter of these results exceed 220 mW m^{-2} (Lawver & Nagihara 1991; Lawver *et al.* 1995). Strong hydrothermal activity, found in the Bransfield Strait in general (Suess *et al.* 1987; Schloesser *et al.* 1988; Dählmann *et al.* 2001; Klinkhammer *et al.* 2001) and, in particular, in the Deception Island area (Somoza *et al.* 2004), confirms the presence of submarine volcanic activity. The central part of the rift graben is only 15–20 km wide and contains several subaerial and submarine volcanoes on a line between the Deception and Bridgeman Islands. They represent the only visible part of a large ∼300-km-long submarine ridge, formed since the Pleistocene by opening of the Bransfield Strait (Weaver *et al.* 1982; González-Ferrán 1985). The most recent eruptions of 1967, 1969 and 1970 at Deception Island (Baker *et al.* 1969; Birkenmajer 1987; Smellie 1988, 1989), as well as permanent seismic activity (Pelayo & Wiens 1989), confirm that tectono-volcanic activity along the Bransfield Strait is still active. Basalts dredged from the volcanoes of the Bransfield rift have transitional affinity between magmas of a standard Pacific backarc basin and depleted upper mantle mid-ocean ridge basalts (Keller *et al.* 2002). In the latter case, melting that resulted in basalt magmas occurred at shallow depths due to the rising and adiabatic decompression of an asthenosphere diapir (Sushchevskaya *et al.* 2002).

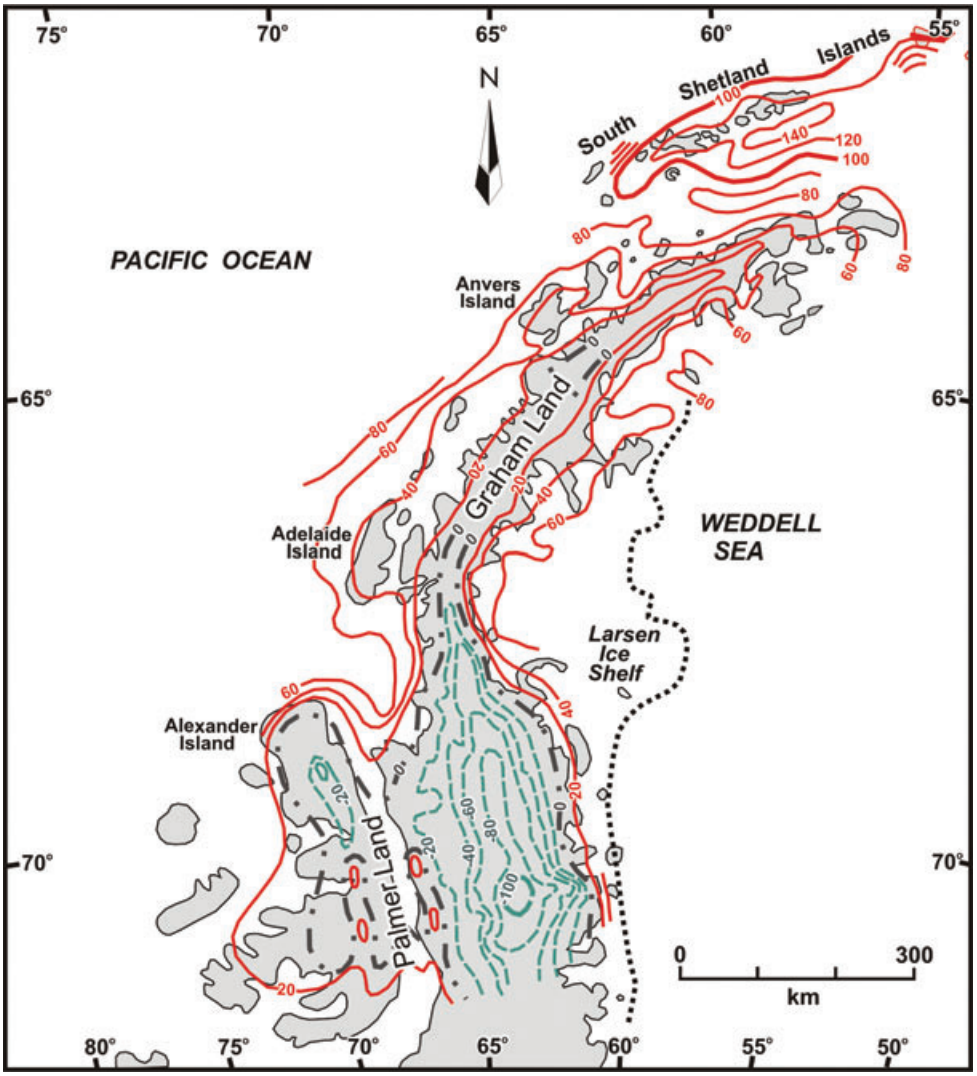

Figure 3. Map of Bouguer gravity anomalies for the Antarctic Peninsula (Renner *et al.* 1985). Red isolines – positive, green – negative, black lines – zero isolines. Values in mGal.

3 GRAVITY ANOMALIES

A regional Bouguer anomaly map of the AP (Fig. 3) was constructed from the data of the gravity surveys carried out by the British Antarctic Survey (Renner *et al.* 1985). The pattern of the Bouguer anomalies shows three main domains. The first domain includes the South Shetland Islands (anomalies up to 120 mGal), the Bransfield Strait (80–140 mGal) and the northern termination of the AP with Bouguer anomalies of 60–80 mGal. The second area characterizes Graham Land—part of the AP and its shelf, which extends between Anvers Island on the north and Adelaide Island on the south. Here Bouguer anomalies over the AP are of 20–40 mGal. They are surrounded on both sides by linear belts of highs reaching 80 mGal on the western shelf and 60 mGal on the east, within the Larsen Ice Shelf. The third domain includes Palmer Land and Alexander Island with broad negative anomalies. These anomalies reach amplitudes of −80 to −100 mGal over Palmer Land and −20 mGal over Alexander Island. Westwards, on the AP shelf the gravity anomalies reach values of 20–40 mGal (Fig. 3). The gravity anomaly field in the region of Palmer Land has been much better delineated from new airborn gravity data (Ferraccioli *et al.* 2006), which indicate the AP batholith as a composite magmatic arc terrane.

For the present 2-D gravity analysis we used the satellite-derived Free-Air gravity anomalies (Sandwell & Smith 1997), which in our study area show rather good correspondence (in order of 6 mGal) with marine gravity anomalies (Sandwell 1992). The northwestern part of the AP shelf is distinguished by belts of high-amplitude highs and lows (Fig. 4). Linear gravity lows image the deep-water trench system along the Pacific margin of the AP. Minimal values of Free-Air anomalies (−100 mGal) are observed along the South Shetland Trench—a deep-water (∼5 km) trough floored by a thick sedimentary wedge and lying on strike with gravity highs. We distinguish a belt of gravity highs over the AP shelf reaching >100 mGal in amplitude above the South Shetland Islands. These gravity highs have been previously interpreted as being caused by high-density bodies of large plutons which constitute the magmatic arc of the Pacific continental margin (Renner 1980; Renner *et al.* 1985; Garrett & Storey 1987). The density of these bodies, which extend down to a depth of 10–20 km, was estimated by Garrett (1990) in the range 2.8–3.0 g cm^{-3} that correspond to a bulk density gabbro-anorthositic composition (Christensen & Mooney 1995).

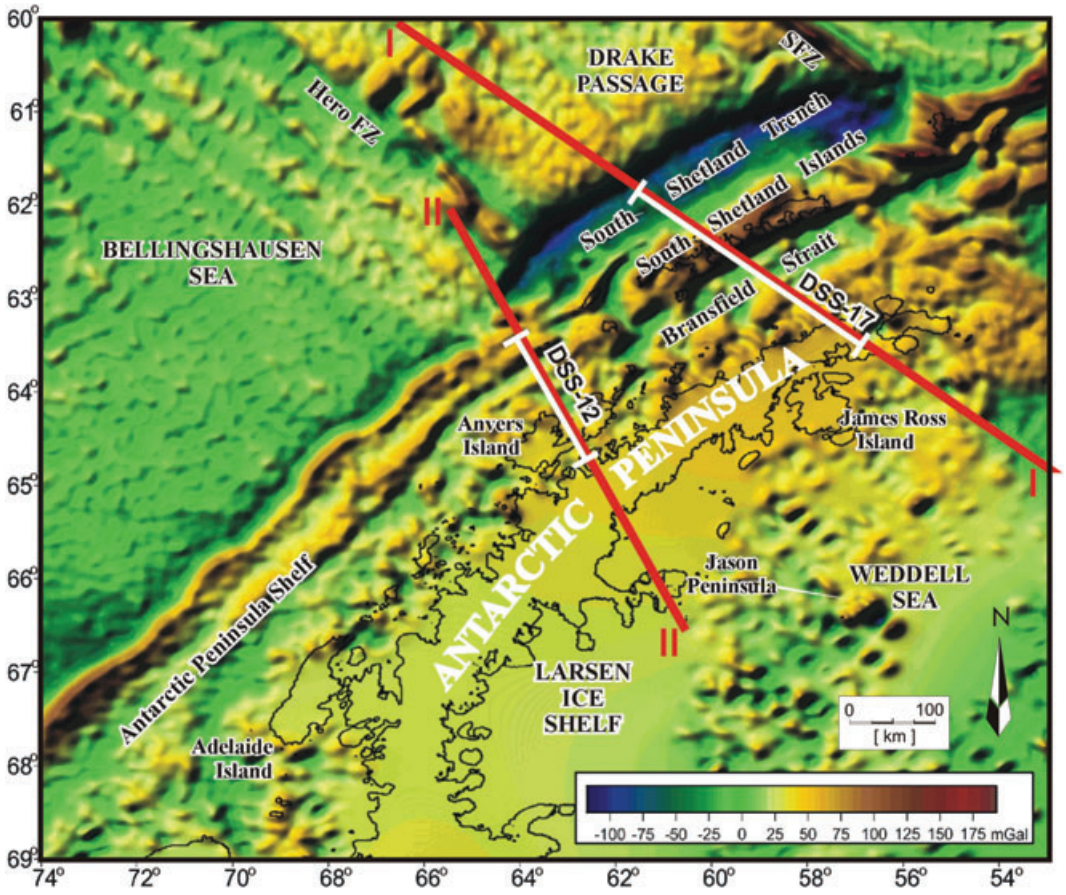

Figure 4. Map of satellite-derived Free-Air anomalies (Sandwell & Smith 1997) over the Antarctic Peninsula region and location of our modelling profiles (red solid lines).

4 MAGNETIC ANOMALIES

Fig. 5 shows anomalies of total magnetic field intensity (TMI, Golynsky *et al.* 2001) used for this study. The continental margin of the AP is marked by a wide (nearly 120 km in width) belt of strong magnetic anomalies. This is the so-called Pacific Margin Anomaly (PMA, Maslanyj *et al.* 1991) or West Coast Magnetic Anomaly (WCMA, recognized by Renner *et al.* 1982)—an arcuate belt of positive magnetic anomalies that extends 3800 km from the South Orkney Island to Thurston Island. The magnitude of the PMA reaches 700 nT in the region of the South Shetland Islands. The PMA overlies the western part of the AP magmatic arc and is comparable to anomalies observed over the Kitakami batholith in Japan (Finn 1994) and the Peninsular Ranges batholiths in California and Baja California (Ferraccioli *et al.* 2006). In the northern part of the AP, between Anvers Island and the northern termination of the Bransfield Strait, the PMA splits into two branches—the western anomaly of high magnitude and eastern anomaly of lower intensity (Fig. 5; Johnson 1999).

The PMA is assumed to be caused by strong magnetization of a chain of batholiths, which were formed in the subduction environment at the shelf zone of the Mesozoic–Cenozoic magmatic arc of the AP (Renner *et al.* 1985; Garrett 1990). Magnetite-bearing gabbro and diorites are the main rock types composing the batholiths. A correlation was found between the PMA positive anomalies and exposures of gabbro and granites in the northern (Johnson 1996) and southern (Johnson & Swain 1995) parts of the study region. In addition, linkage of the magnetic anomaly of 500 nT with exposures of gabbro was established in the Pitt Islands. A good correlation is also observed on the islands of Anvers, Bride, Horseshoe and Terra Firma. Calculations performed by Johnson (1999) show that the PMA can be explained by bodies with apparent magnetic susceptibility of 0.055–0.075 SI and lower bounds occurring at the depth of nearly 20 km, the estimated depth of the Curie isotherm. Depths to the upper surface of the source bodies for the PMA vary from 0 to 6 km. Apparent magnetic susceptibility values used for modelling correspond well with the measured susceptibility of rock samples of the gabbro-diorite group of the AP, ranging from 0.01 to 0.23 SI (Table 1; Maslanyj *et al.* 1991; Johnson 1996; Vaughan *et al.* 1998). Vaughan *et al.* (1998) also suggested that the PMA in Palmer Land may have been associated with an intense phase of tonalitic plutonism in the early Cretaceous. Magnetic modelling performed by Garrett (1990) indicates the PMA to be caused by the effect of bodies in the upper-middle crust of about 2 A m^{-1} magnetization; the highest magnetization (2.6 A m^{-1}) was determined for the South Shetland Islands and Drake Passage section.

A marine magnetic survey carried out in the Bransfield Strait revealed positive anomalies varying from 200 to 2000 nT and interpreted as arising from intrusions of basalt dikes along a ridge axis (Kim *et al.* 1992). Gràcia *et al.* (1996) correlated positive magnetic anomalies (300–400 nT) with a chain of large volcanoes.

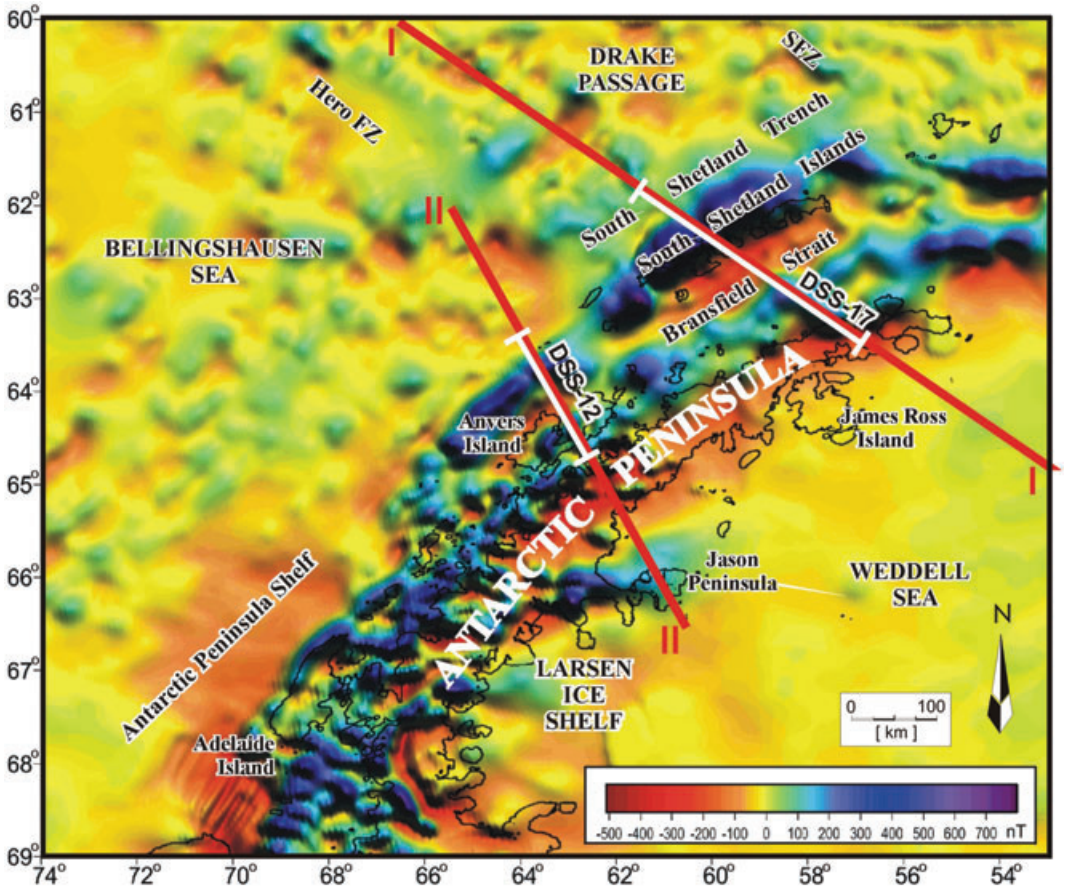

Figure 5. Total field magnetic anomaly map for the Antarctic Peninsula region (Golynsky *et al.* 2001) and location of our modelling profiles (red solid lines).

5 SEISMIC REFRACTION STUDY, VELOCITY MODELS AND MOHO MAP

In the transition zone between the Drake and South Shetland microplates and the Antarctic Plate, 20 deep seismic sounding profiles were performed during the Polish Geodynamic Expeditions (Fig. 6a). The interpretation yielded 2-D models of the crust and upper mantle down to 80 km depth. Seismic refraction and wide-angle reflection measurements were done using explosions in the sea along profiles of a total length of about 4000 km. Shots of between 25 and 120 kg of TNT were electrically detonated in the sea from the ship at a depth of 70–80 m. The distances between shots were 1–5 km. All shots were recorded by three and five channel vertical component seismic stations located on land (Guterch *et al*. 1998). The shots along profile DSS-20 in the Bransfield Strait were recorded by ocean bottom seismometers (OBSs; Grad *et al*. 1997). Seismic refraction records obtained in the area of the AP show a complicated seismic wavefield, resulting from large variations in seafloor depth, large subsurface velocity structures in the sedimentary cover, presence of intracrustal intrusions and Moho topography.

The 310-km-long profile DSS-17 carried out in 1987 runs from the South Shetland Trench through the South Shetland Islands and Bransfield Strait and terminates at the AP (Trinity Peninsula, Figs 2, 6a; Grad *et al.* 1993a,b). 30 shots were fired in the sea. Seismic waves from explosions were recorded by analogue seismic instruments on four land stations: two in the South Shetland Islands (AP — the Arturo Prat station at Greenwich Island, HM — a station at Half Moon Island) and two at the AP (HB — at the Hope Bay, OH — station O'Higgins).

Large apparent velocities are indicative of the presence of seismic boundaries that strongly dip from the Drake Passage under the South Shetland Islands. The complicated pattern of the seismic wavefield on profile DSS-17 is indicative of the complex structure of the crust and subcrustal lithosphere. Fig. 7(a) represents a new version of the velocity model on the DSS-17 profile presented by Grad *et al.* (1993a,b). A new model has been prepared for this paper, based on interpretation of seismic profiles (e.g. DSS-20) shot in the Bransfield Strait region (Janik 1997a, b). According to the velocity model in Fig. 7(a), the depth of the Moho boundary ranges from 10 km for the oceanic crust below the Drake Passage and the South Shetland Trench area to about 40 km under the AP. The sub-Moho V_p velocities of 8.3 km s^{-1} are a little higher than in previous models. This value is comparable to the velocity of 8.4 km s^{-1} found by Contreras-Reyes *et al.* (2008) offshore in the subduction zone in Chile. The velocity structure reveals several individual blocks in the crust. In the oceanic domain a sequence of strata with velocities ranging from 2.0 to 5.6 km s^{-1} overlies the 4–5-km-thick layer of crystalline crust with approximately 6.9 km s^{-1} velocity. In the South Shetland Islands block the low-velocity sedimentary complex (2.0–4.0 km s^{-1}) covers three crystalline crust complexes with V_p of 5.6–6.1 km s^{-1}, 6.4–6.8 km s^{-1} and more than 7.2 km s^{-1}. The crustal structure beneath the Bransfield Strait is highly anomalous. A specific feature of this is a high-velocity body with *P*-wave velocities >7.0 km s^{-1}, detected in the 15–30 km depth interval. This high-velocity body thickens northwestwards

Table 1. Physical properties of rock complexes of Antarctic Peninsula.

Complexes	Rock composition	Density (g cm^{-3})		Velocity (km s^{-1})				Magnetic parameters			Comments
		N	ρ	N	V_p	V_s	V_p/V_s	N	Susceptibility æ, (SI)	N	NRM (A m^{-1}) (A m^{-1})	
Mesozoic–Cenozoic volcanic rocks	Andesite, basalt, diabase	67	2.53–2.94 **2.78**					96	0.001–0.12 **0.037**	90	0.002–2.85 **0.41**	*
	Basalt, andesite, rhyolite	131	**2.70**					40	**0.017**			Garrett (1990)
	Rhyolit, dacite	16	2.66–2.83 **2.71**	15	5.42–6.05 **5.72**	3.15–3.52 **3.34**	1.60–1.72 **1.68**	16	**0.016**			Lebedev *et al.* (2002)
	Andesite, basalt, dolerite	20	**2.88**	20	5.66–6.35 **5.90**	3.20–3.56 **3.41**	1.60–1.84 **1.72**	18	0.016–0.133 **0.044**			Lebedev *et al.* (2002)
Mesozoic–Cenozoic plutonic rock complex	Granodiorite, granite	106	2.61–2.85 **2.71**					106	0.002–0.084 **0.035**	67	0.033–1.07 **0.366**	*
	Granite	91	**2.62**					93	**0.008**			Garrett (1990)
	Granodiorite	9	**2.69**									Garrett (1990)
	Diorite, granodiorite	136	**2.72**					128	**0.020**			Garrett (1990)
	Granite	5	2.59–2.64 **2.61**	5	4.90–5.16 **5.01**	2.90–3.14 **3.06**	1.56–1.72 **1.64**	5	**0.016**			Lebedev *et al.* (2002)
	Granodiorite	7	2.61–2.72 **2.65**	7	4.78–5.62 **5.24**	2.84–3.16 **3.09**	1.63–1.79 **1.69**	7	0.016–0.033 **0.022**			Lebedev *et al.* (2002)
	Diorite	10	2.70–2.82 **2.75**	10	5.39–5.82 **5.63**	3.22–3.45 **3.34**	1.63–1.74 **1.69**	10	0.024–0.140 **0.061**			Lebedev *et al.* (2002)
	Gabbro, gabbro-anorthosites	83	2.74–3.17 **2.86**					82	0.001–0.25 **0.064**	79	0.06–9.3 **1.93**	*
	Gabbro	49	**2.84**					93	**0.033**	14	0.02–10.9 **2.3**	Garrett (1990)

Note: N indicates the number of samples, numbers above the line show data range (from minimal to maximal values), while bold numbers indicate the average value of the parameter. The * label marks the data collected during Ukrainian Antarctic expeditions.

and below the South Shetland Islands it extends from a depth of 5–40 km, that is, to the base of the crust. In the AP, crystalline crust layers of about 5.3–6.0, 6.7 and >7.0 km s^{-1} have been distinguished.

In the transition zone from the Drake Passage to the South Shetland Islands a seismic boundary in the lower lithosphere occurs at a depth ranging from 35 to 80 km (Fig. 7a). The dip of both the Moho and this seismic reflector is approximately 25° and indicates, probably, the direction of subduction of the lithosphere of the Drake Plate under the Antarctic Plate.

The seismic study of the Bransfield Strait was continued in 1990–1991 during the first detailed seismic refraction study (Grad *et al.* 1997) using five OBS along a 310-km-long seismic profile DSS-20 running along the Bransfield Rift axis (Fig. 6a) from southwest (in the vicinity of Deception Island) to northeast (in the vicinity of Bridgeman Island). The crustal velocity section on this profile shows three blocks (Grad *et al.* 1997) describing the crustal structure of western, central and eastern sub-basins of the Bransfield Rift. A high-velocity body with V_p = 7.4–7.7 km s^{-1} has been revealed from these studies at the depth of 15–32 km beneath the central subbasin in the Bransfield Strait. Detailed images of its shape from the DSS data were shown by Janik (1997a,b) and Janik *et al.* (2006). It is interpreted as magmatic material underplated to the crust during rifting. An upper mantle with velocities >8.0 km s^{-1} was observed at a depth 30–32 km along the DSS-20 profile, thus indicating the presence of continental crust below the Bransfield Rift. Ashcroft (1972) and Davey (1972) had suggested the existence of a semi-oceanic crust beneath the Bransfield Strait. Seismic experiments on profile DSS-20 have shown an absence of oceanic crust. Later wide-angle seismic surveys, consisting of a grid of eight dip profiles, conducted in Bransfield Strait in 2000 (Barker *et al.* 2003; Christeson *et al.* 2003) revealed a similar pattern along the profiles DSS-17 and DSS-20, and high *P*-wave velocities (>7.25 km s^{-1}) at a depth of 10–15 km below the central part of Bransfield Strait, which they interpreted as the Moho boundary. In Fig. 7(a) it corresponds to the top of the high-velocity body.

Seismic profile DSS-12 was one of seven profiles acquired during 1984–1985 (Środa *et al.* 1997) within the continental margin of the AP between the Palmer Archipelago and Adelaide Island. Profile DSS-12 of 160 km length crosses the AP shelf from Anvers Island to the edge of the continental margin (Figs 2, 6a). 15 shots were fired in the sea with distances between shot points of about 6 km. Very good recordings were obtained along the profile and this allowed a detailed study of the seismic wavefield and crustal structure (Środa *et al*. 1997). The final velocity model along the profile DSS-12 is shown in Fig. 7(b). In the area adjacent to the AP, a thin sedimentary cover of 0.2–1.5 km thickness was found, whereas in the western part of the study area a sedimentary basin with a thickness up to 3 km is observed. *P*-wave velocities of 4.4–5.2 km s^{-1} were assumed for sediments. In the upper crust, *P*-wave velocities of 6.35 km s^{-1} were found at a shallow depth (less than 1 km) in a wide belt along the AP. *P*-wave velocities of about 6.6 km s^{-1} were found below 5–15 km depth. The crystalline crust consists of three parts, with velocities of 6.3–6.4, 6.6–6.8 and 7.1–7.2 km s^{-1} (Fig. 7b). The thickness of the crust varies from 36 to 42 km, and maximum thickness is observed below Anvers Island. Moho shallowing up to about 22 km is observed towards the Pacific Ocean (Środa *et al.* 1997).

Results of deep seismic profiles were synthesized to produce a map of Moho depth beneath the NW coast of the AP (Fig. 6b, Guterch *et al.* 1998; Janik *et al.* 2006). The map shows that the maximum crustal thickness of 38–42 km occurs along the AP shelf between Adelaide Island and the Palmer Archipelago. Towards the

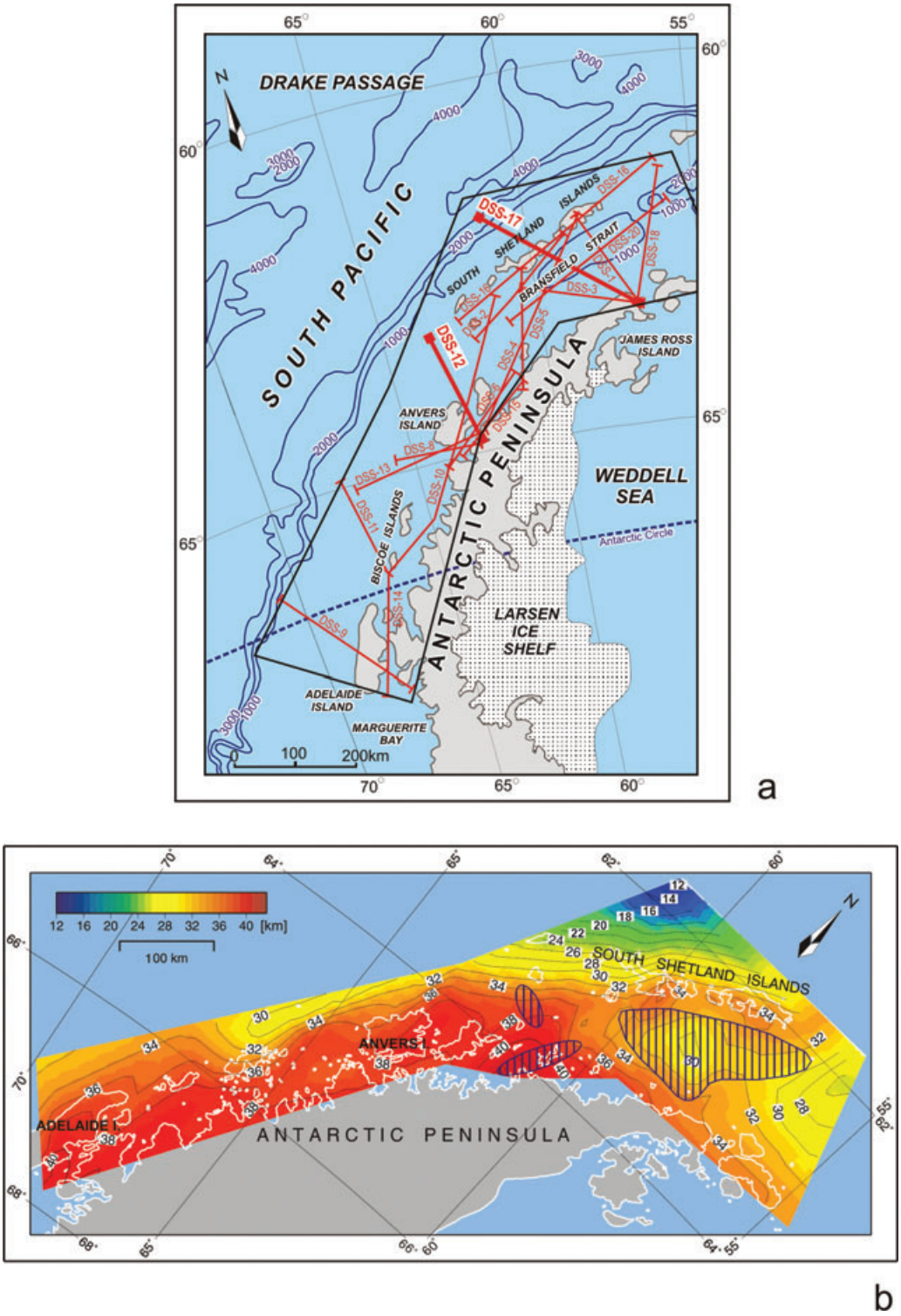

Figure 6. Location of deep seismic sounding (DSS) profiles (a) in Antarctic Peninsula Shelf (Guterch *et al.* 1998) and map of the depth to the Moho boundary (b) along the Antarctic Peninsula, based on data from ray-tracing models of the crustal structure (Janik *et al.* 2006). Thick lines in (a) indicate the DSS-12 and DSS-17 profiles used for 2-D gravity and magnetic modelling. Blue hatched areas in (b) over the central part of the Bransfield Strait mark the extent of the high velocity anomaly, where at a depth of 13–18 km *P*-wave velocities reach 7.2 km s^{-1}, as well as the extent of two other areas of anomalously high velocity.

Pacific Ocean, the Moho depth decreases and reaches 30–32 km at the edge of study area. The dipping Moho boundary indicates the occurrence of a transition zone between the oceanic Pacific crust and the continental crust of the AP. In the Bransfield Strait area, the depth of the Moho discontinuity increases from about 12 km for the oceanic crust of the Phoenix Plate to about 25 km for the South Shetland Islands shelf, and 30–33 km for the South Shetland Islands crustal block. In contrast, the AP and its adjacent shelf have a typical continental crustal thickness of 36–45 km. The Moho depth beneath the Bransfield trough is about 30–32 km.

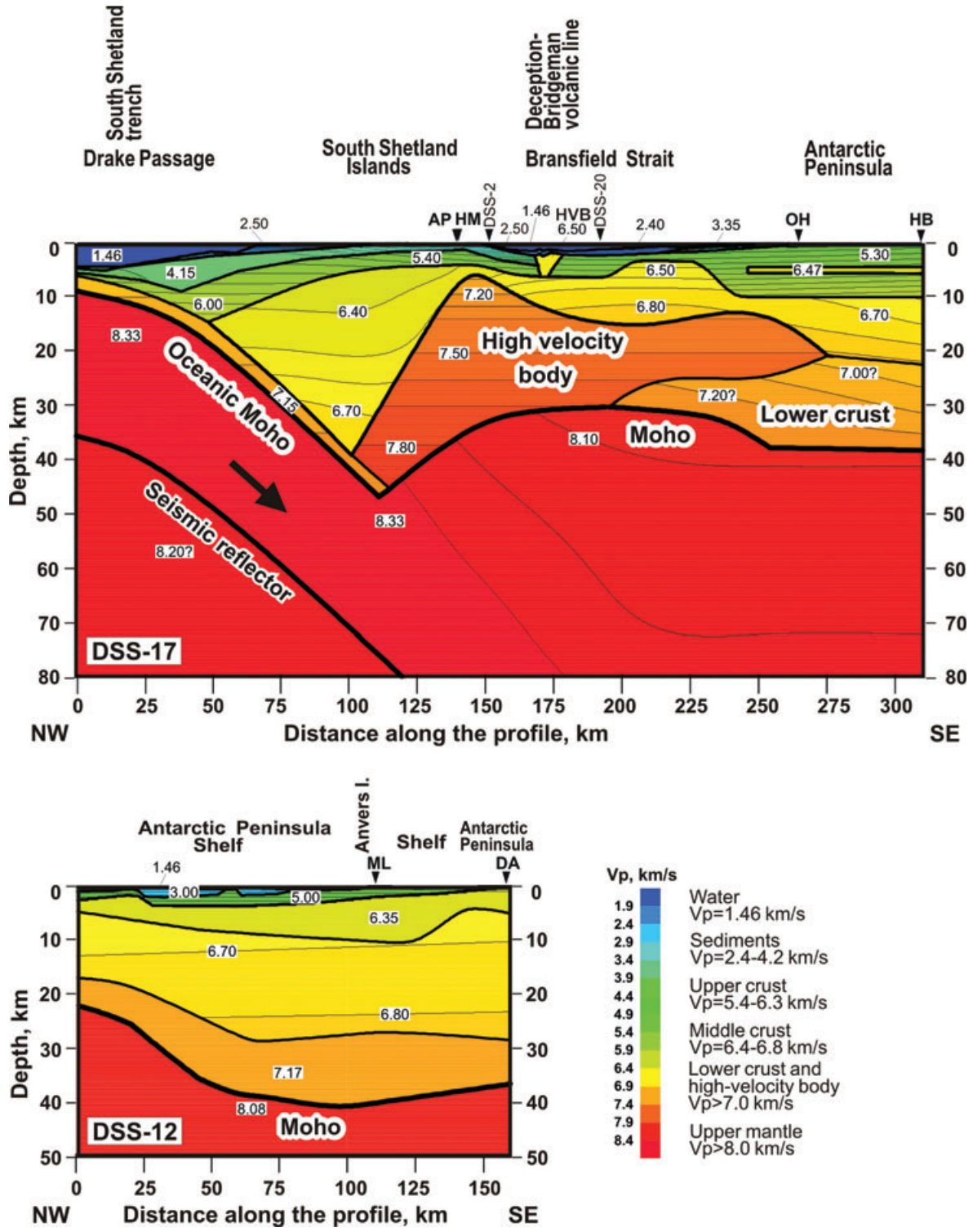

Figure 7. Velocity models along the DSS-17 line (a), modified from Grad *et al.* (1993a,b) and Janik (1997a,b) and DSS-12 line (b) (Środa *et al.* 1997). Location of the profiles is shown in Figs 2 and 6(a). Numbers indicate *P*-wave velocity in km s^{-1}.

6 PHYSICAL PROPERTIES AND PARAMETERIZATION OF THE INITIAL MODELS

Data on the distribution of physical properties of the main rock complexes of our study region are used for parameterization of initial gravity and magnetic models and also for interpretation of final models. The bulk of rocks exposed on the islands of the AP shelf and mainland are made of plutonic rocks of the AP batholith (Leat *et al.* 1995) and volcanic rocks of the AP Volcanic Group (Thompson & Pankhurst 1983). The plutonic rocks that form the AP batholith were emplaced over the period ~240 to 10 Ma with an Early Cretaceous peak of activity (Leat *et al.* 1995). Early Cretaceous plutonic rocks of gabbro-granite composition (with a prevalence of diorites)

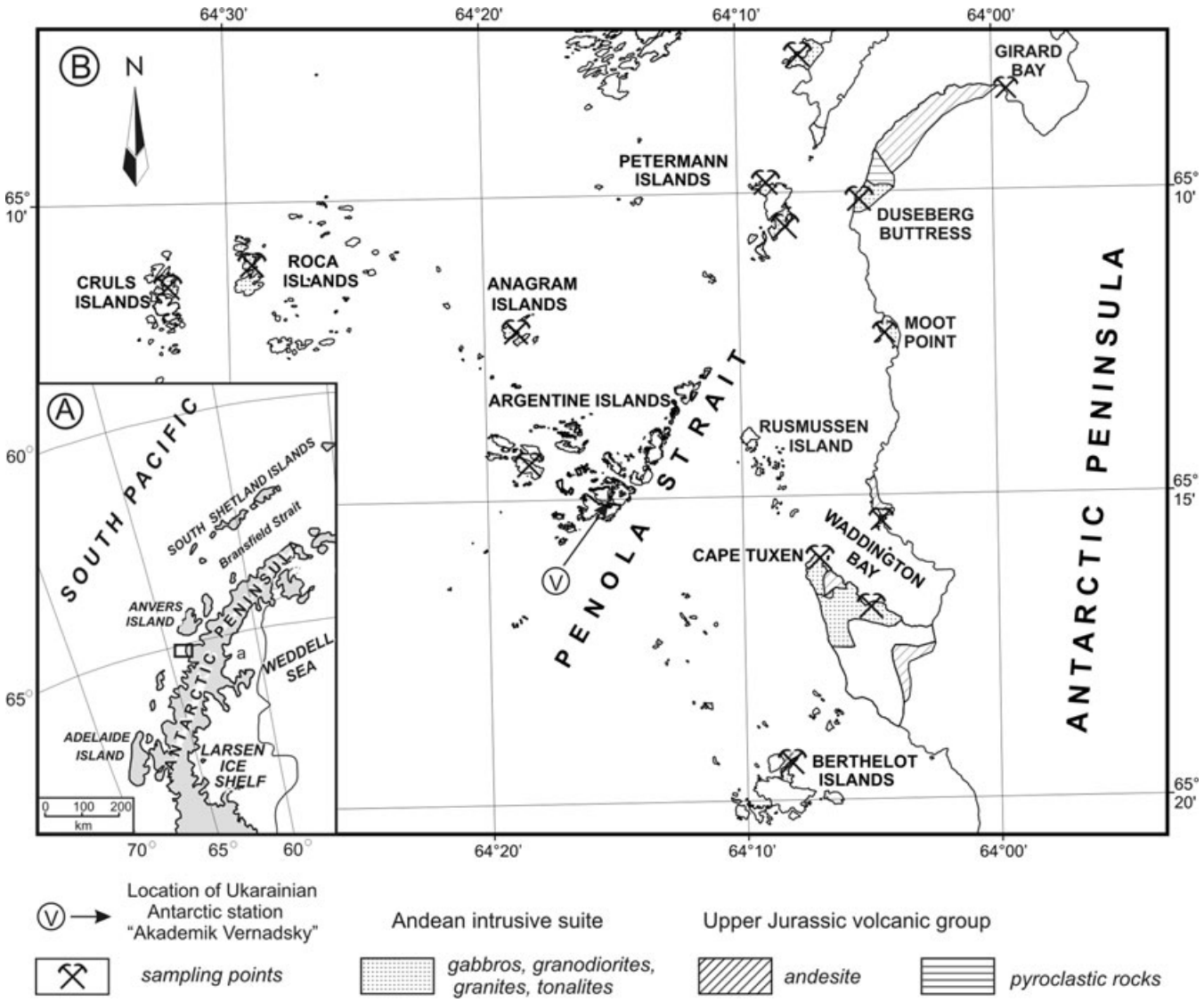

Figure 8. Location of rock samples in the Argentine Islands area (b), shown by a small rectangle on the Antarctic Peninsula map (a); the V symbol indicates the location of Ukarainian Antarctic station 'Akademik Vernadsky' (65°5′S, 64°6′W).

constitute the widespread plutons and batholiths (Willan & Kelley 1999; Leat *et al.* 1995). The volcanic rocks of the AP Volcanic Group, which occur as veins, dykes and flows, are represented by andesites, diabases, basalts, rhyolites, dolerites, and dacites (Weaver *et al.* 1982; Riley *et al*. 2001).

During Ukrainian Antarctic expeditions (1998–2008), collections of rock samples, exposed on the archipelago of the Argentine Islands (in the region of Ukrainian Antarctic station 'Akademik Vernadsky' shown by V mark in Fig. 8) and adjoining the western coast of the AP, were gathered for petrophysical study. The location of rock samples is shown in Fig. 8. The results of this study are summarized in Fig. 9 and Table 1 (marked by $*$ in the comment). For comparison Table 1 includes also data from previous studies undertaken by the British Antarctic Survey (Garrett 1990) and Ukrainian Antarctic expeditions (Lebedev *et al.* 2002).

Two groups can be distinguished amongst the volcanic rocks. The first group, defined by lowest values of physical parameters, includes rhyolites, dacites, andesites with average density $\rho = 2.7$ g cm^{-3} and magnetic susceptibility æ $= 0.017$ SI (Garrett 1990; Lebedev *et al.* 2002). The second group of more mafic composition comprises diabases, basalts, dolerites and andesites with densities 2.84–2.90 g cm^{-3}, whereas average values of both æ and natural remanent magnetization NRM increase to 0.04 SI and 0.41 A m^{-1}, respectively (Fig. 9 and Table 1). The latter group includes also volcanic rocks of very high NRM values. They are basalts of Cape Tuxen (NRM $=$ 2.1–4.2 A m^{-1}) and dolerites of Argentine Islands (Fig. 8) with NRM $=$ 0.2–0.7 A m^{-1} (Lebedev *et al.* 2002). The two groups of volcanic rocks also differ in seismic velocities: increased V_p values (to 5.9 km s^{-1}) are attributed to mafic volcanic rocks (Table 1).

Granitoids of the AP batholith (Leat *et al.* 1995) are represented mostly by granodiorites and, to a lesser extent, by granites, which usually comprise one group under the joint name 'granodiorites'. Heterogeneity of this group is revealed by a bi-modal density histogram (Fig. 9) with two peaks characterizing the granites and granodiorites with densities 2.61–2.62 and 2.69–2.72 g cm^{-3}, respectively (Table 1). Average values of æ range from 0.016 SI in granites to 0.020–0.022 SI in granodiorites, whereas the NRM of the latter is 0.366 A m^{-1} (Table 1). Increased values of æ (0.035 SI) obtained for the granodiorites of our collection (marked by * in Table 1) could

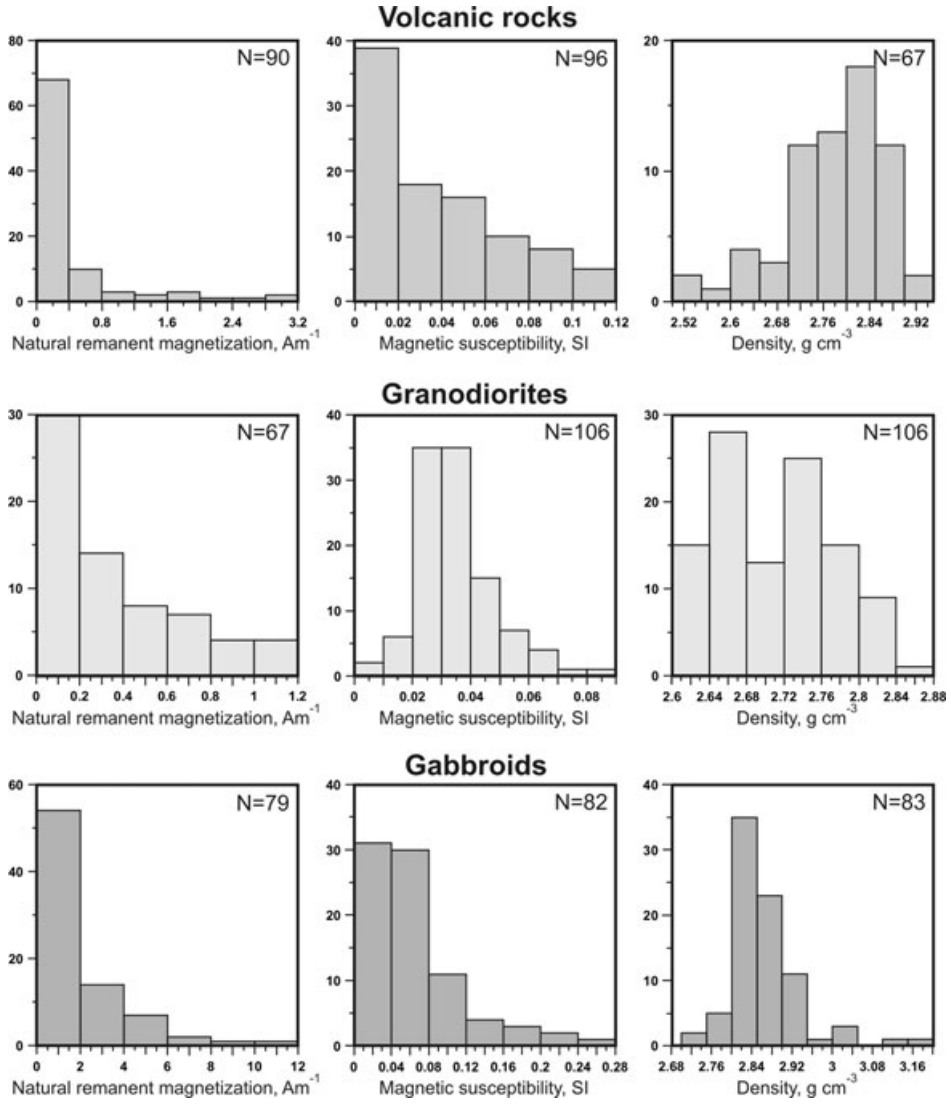

Figure 9. Diagrams of physical properties (magnetic parameters and density) of main rock complexes exposed on the Argentine Islands and adjoining western coast of Antarctic Peninsula. Diagrams have been compiled from the data in Table 1 (marked by ∗ in the comment).

be explained by a prevalence in the dataset of granodiorites of the archipelago of the Argentine Islands and adjoining part of the AP coast, which could have higher magnetization.

Gabbroids of the AP batholith are characterized by an average density of 2.84–2.86 g cm^{-3} (Table 1 and Fig. 9; Garrett 1990). The distinction in average æ of these rocks, estimated to be 0.064 SI and 0.033 SI according to the data of Ukrainian expeditions and British Antarctic Survey (Garrett 1990), respectively (Table 1), could be explained by above mentioned tendency observed for granodiorites, that is, by a prevalence in the dataset of rocks of the archipelago of Argentine Islands. In addition, diorites with average æ = 0.061 SI could also be associated with this group (Table 1; Lebedev *et al.* 2002). Average NRM = 1.9 A m^{-1} of gabbro and gabbro-anorthosites (estimated on 79 samples, Table 1) is in good correspondence with previous estimates (2.0–2.3 A m^{-1}; Garrett 1990). High magnetization of the gabbro group is caused by high magnetite content, reaching 12 per cent (Goldring 1962; Artemenko *et al.* 2009). These rock types are exposed on Argentine Islands, Central Hugo Islands and other localities within the Graham Land and constitute bodies and plutons of the large AP batholith. The highest magnetite content, up to 30 per cent, was obtained in gabbroids exposed on Anagram Island and Cape Tuxen of the AP (Fig. 8; Artemenko *et al.* 2009).

The density values of main rock types (Table 1 and Fig. 9) were used to constrain the upper and mid-crust intervals of the initial density model. To constrain the density model for the entire crust and upper mantle, we also used conventional velocity/density conversion functions. Table 2 and Fig. 10 show the densities for different complexes and layers estimated from the Nafe-Drake (Nafe & Drake 1963) and the Birch empirical functions between V_p and density (Birch 1960, 1961). These estimates incorporate velocities taken from seismic models in Fig. 7.

7 DENSITY MODEL OF THE CRUST AND UPPER MANTLE ACROSS DRAKE PASSAGE AND BRANSFIELD STRAIT TO THE ANTARCTIC PENINSULA

A joint gravity and magnetic model on line I-I of 860 km total length was set along the seismic profile DSS-17 crossing the study region in the area of South Shetland Trench and Islands and Bransfield Strait

Table 2. Density values used in the 2-D modelling of the Antarctic Peninsula continental margin.

	Layer	*P*-wave velocity from seismic models in Fig. 7 V_p (km s^{-1})	Density for models in Figs 11–12, ρ (g cm^{-3})	Magnetic susceptibility for models in Figs 11–12, æ (SI)
Sediments	Oceanic sediments of the Drake Passage	2.4–3.1	1.8–1.9	
	Sediments of accretionary complex	3.8–4.5	2.10–2.30	
Crust	Metasedimentary rocks of basement and intercalated volcanics; upper 'granitic' crust of the Antarctic Peninsula	5.1–6.0	2.5–2.62	0.02
	Upper 'granodioritic' crust of the Antarctic Peninsula	6.3–6.45	2.73–2.77	0.035
	Middle crust of the Antarctic Peninsula	6.5–6.85	2.85–2.87	
	Lower crust of the Antarctic Peninsula	7.10–7.20	3.0	
	High-velocity body in the lower crust of the Bransfield Strait, crustal batholith of the South-Shetland Islands	7.20–7.70	3.05	0.07
	Oceanic crust of the Drake passage and the Bellinsghausen Sea	6.9–7.2	2.9	
Upper mantle	Continental uppermost mantle of the Antarctic Peninsula	8.1	3.25–3.30	
	Lithospheric mantle of the Drake Passage and the Bellinsghausen Sea	8.3	3.3	
	Upper mantle beneath the South-Shetland islands–Bransfield Strait	8.1	3.18	

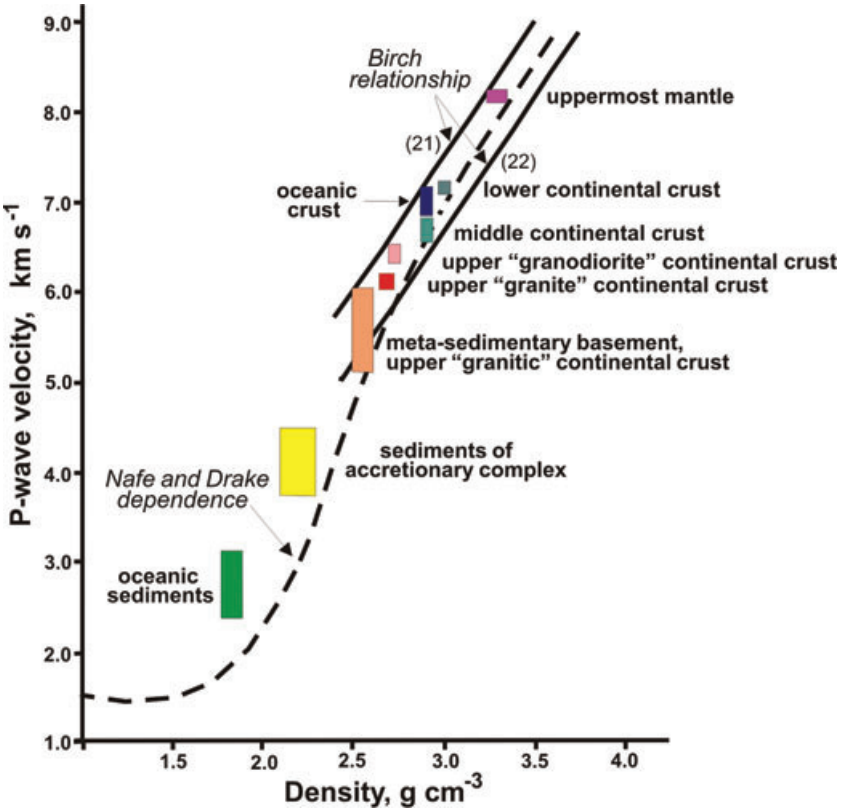

Figure 10. Diagram of the density–velocity relation for sediments, crystalline crust and uppermost mantle (shown also in Table 2) for the Antarctic Peninsula margin, used for the gravity modelling. The velocity values were taken from the seismic observations along seismic profiles shown in Fig. 7. The density values were constrained by these velocity observations and estimated from Nafe-Drake (dashed line) and Birch (solid lines, shown for atomic mass 21 and 22) conversion functions.

(Figs 6a and 7a). A seismic section along the nearly perpendicular line DSS-20 that traversed along the rift axis (Grad *et al.* 1997) was also taken into account. Thus, the central part of the line I-I, which is one third of the whole line length, was elucidated by seismic data from DSS-17 and DSS-20, whereas the crustal structure on both sides of it was constructed by 2-D gravity and magnetic modelling. For the modelling we used satellite-derived Free-Air gravity and aeromagnetic anomalies (Figs 4 and 5).

For gravity computations we used the software developed for 2-D and 3-D modelling (Tchernychev & Makris 1996), which is based on the Talwani *et al.* (1959) algorithm. The models were approximated by prisms of 2×0.25 km^2 (X, Z) size, defining the areas of constant density. For gravity calculations the software uses relative densities, obtained by normalizing the absolute density values to some reference density. For this parameter the program uses a constant value representing the average density for an average column of the model from the surface to the base of the model. Calculation of the density model indicates this average density parameter to be equal to 3.04 g cm^{-3}. The software provides also for calculations of gravity inversion formulated by a linear approach (estimation of density for known geometry). This is especially useful for density range estimates in the parts of the model, which are poorly constrained by seismic data and for the upper mantle. 2-D magnetic modelling was performed by Mag2dc software (Cooper 1997) using the set of separate bodies of arbitrary configuration. Mag2dc allows forward modellling and inversion of magnetic data. The magnetic bodies are placed in the upper-middle crust interval bounded below by the Curie isotherm, which has been estimated for the AP continental margin at a depth of approximately 20 km (Johnson 1999). The geometry of the initial models was constrained by velocity models in Fig. 7. Density parameterization of the sections was made by conversion of *P*-wave velocities of the seismic models (Fig. 7) into densities using the conversion function in Fig. 10. In addition, for the upper part of the section we used laboratory measured physical properties of major rock types that outcrop on the islands and mainland of the AP (Fig. 9 and Table 1). Further refinement of the models was achieved with a better fit between calculated and observed potential fields by means of changing the densities and susceptibilities in the layers and bodies of the model.

The final density model on line I-I is shown in Fig. 11. It is fitted with 10 mGal of average deviation between the calculated and observed fields that is about 6 per cent of the maximum variation of the Free-Air anomalies along the profile. The model in Fig. 11 consists of three main domains—the continental crust of the AP and Larsen Ice Shelf (km 630–880), the oceanic block of Drake Passage (km 0–340 km) and, located in between, a transition block. The lattermost characterizes the structure of the crust between the South Shetland Trench and Bransfield Strait.

The thick continental crust of the AP and Larsen Ice Shelf consists of three layers. The upper crust reaches 10 km in thickness and has a density of 2.55–2.62 g cm^{-3}. The middle crust is 12 km thick and is characterized by a density of 2.87 g cm^{-3} and the lower crust has the highest values of velocity and density (>7.0 km s^{-1} and 3.0 g cm^{-3}). The Moho is a flat boundary lying at a depth of 38–40 km with a velocity and density underneath the boundary of 8.10 km s^{-1} and 3.29 g cm^{-3}, respectively.

The oceanic crust of the Drake Passage has typical values for oceanic areas—a thin (5–7 km) crystalline crust of high velocity (6.9 km s^{-1}) and density (2.9 g cm^{-3}) overlain by a thin layer of low-density (1.9 g cm^{-3}) oceanic sediments under a layer of seawater 3–3.5 km thick. Below the Moho, occurring at a depth of 12 km, velocity and density were estimated as 8.3 km s^{-1} and 3.3 g cm^{-3}, respectively. Below the seismic reflector the density was estimated to be 3.16 g cm^{-3} (asthenosphere).

A very complex crustal structure is seen in the transition block, which includes the area between the South Shetland Trench and Bransfield Strait. A spectacular feature of this block is a gravity maximum reaching 110 mGal above the South Shetland Islands (Fig. 11). Our gravity models indicate that this high is caused by a large batholiths that extend from 3 to 20 km depth. The batholiths is of 40 km wide near the surface and has a steep and subvertical western flank, while eastwards it continues as a thinner body that extends into the lower crust below the Bransfield Strait (Fig. 11). The geometry of this body taken from seismic model in Fig. 7(a). The apparent density (3.05 g cm^{-3}) and seismic velocity (>7.2 km s^{-1}) suggest an ultramafic composition for the body. An uplifted crustal wedge with a 2.87 g cm^{-3} density was implaced to the west of the South Shetland batholiths in a subduction environment by slow ongoing subduction of a remnant of Phoenix Plate under the South Shetland Islands. The existence of this uplifted crustal block is also supported by a strong magnetic anomaly of more than 400 nT, which corresponds to the western branch of the PMA. This anomaly is caused by a magnetic body of 80 km width occurring at 3–20 km depth. The high magnetic susceptibility (0.08 SI) and average density (2.87 g cm^{-3}) values (Fig. 11), as shown from the data in Table 1 and Fig. 9, are indicative of a mafic composition of an intrusive rock complex (gabbro-diorites, gabbro, and gabbro-norites).

The gravity low (−60 mGal) of the South Shetland Trench is caused by a thin sequence of low-density oceanic sediments ($\rho =$ 1.8 g cm^{-3} and $V_p = 2.5$ km s^{-1}) and sediments of an accretionary wedge complex ($\rho = 2.15$ g cm^{-3} and $V_p = 4.2$ km s^{-1}). The latter are modelled as being up to 5 km thick 25–30 km to the southeast from the trench axis. In addition, a contribution to this gravity low is made by the sequence of meta-sedimentary rocks of the basement and intercalated volcanics, which are associated with $V_p = 5.5$ km s^{-1} and $\rho = 2.55$ g cm^{-3}. The occurrence of volcanic rocks here corresponds to very high values of apparent magnetic susceptibility (0.10 SI) derived below the South Shetland Trench at a depth of 1–8 km (Fig. 11). This interpretation agrees with measured magnetic susceptibility over five samples of basalts and dolerites exposed on the Argentine Islands, that have susceptibility in the range 0.08–0.13 SI (Lebedev *et al.* 2002).

The same rock complexes seen in the basement are present at a depth of 2–5 km below the Bransfield Strait, where they are overlain by thin sediments (1–4 km thickness) of density 2.10–2.20 g cm^{-3}. These sequences, as it follows from the seismic model in Fig. 7(a), are cut by a small, high-velocity body ($V_p = 6.5$ km s^{-1} and $\rho =$ 2.9 g cm^{-3}) in the form of a volcanic edifice, which is indicated also by a local gravity anomaly of 15 mGal (Fig. 11) and a local magnetic anomaly (Kim *et al.* 1992). These gravity and magnetic anomalies mark the presence of a chain of subaerial and submarine volcanoes along the Bransfield rift axis from the Deception volcano on the south to Bridgeman Island on the north (Gràcia *et al.* 1996). The thinned crystalline crust below the Bransfield rift is highly anomalous. The upper crust of 2.87 g cm^{-3} density contains a magnetic body of 0.07 SI susceptibility responsible for the 250–300 nT magnetic anomaly of the eastern branch of the PMA (Fig. 11). The lower crust body beneath the Bransfield Strait is characterized by $V_p = 7.4$–7.7 km s^{-1} and $\rho = 3.05$ g cm^{-3}. Transition from the thinned crust of the Bransfield Rift to the AP continental crust is distinguished by a local gravity anomaly of 30 mGal caused by a body in the upper crust (at 5 km depth) with 2.83 g cm^{-3} and

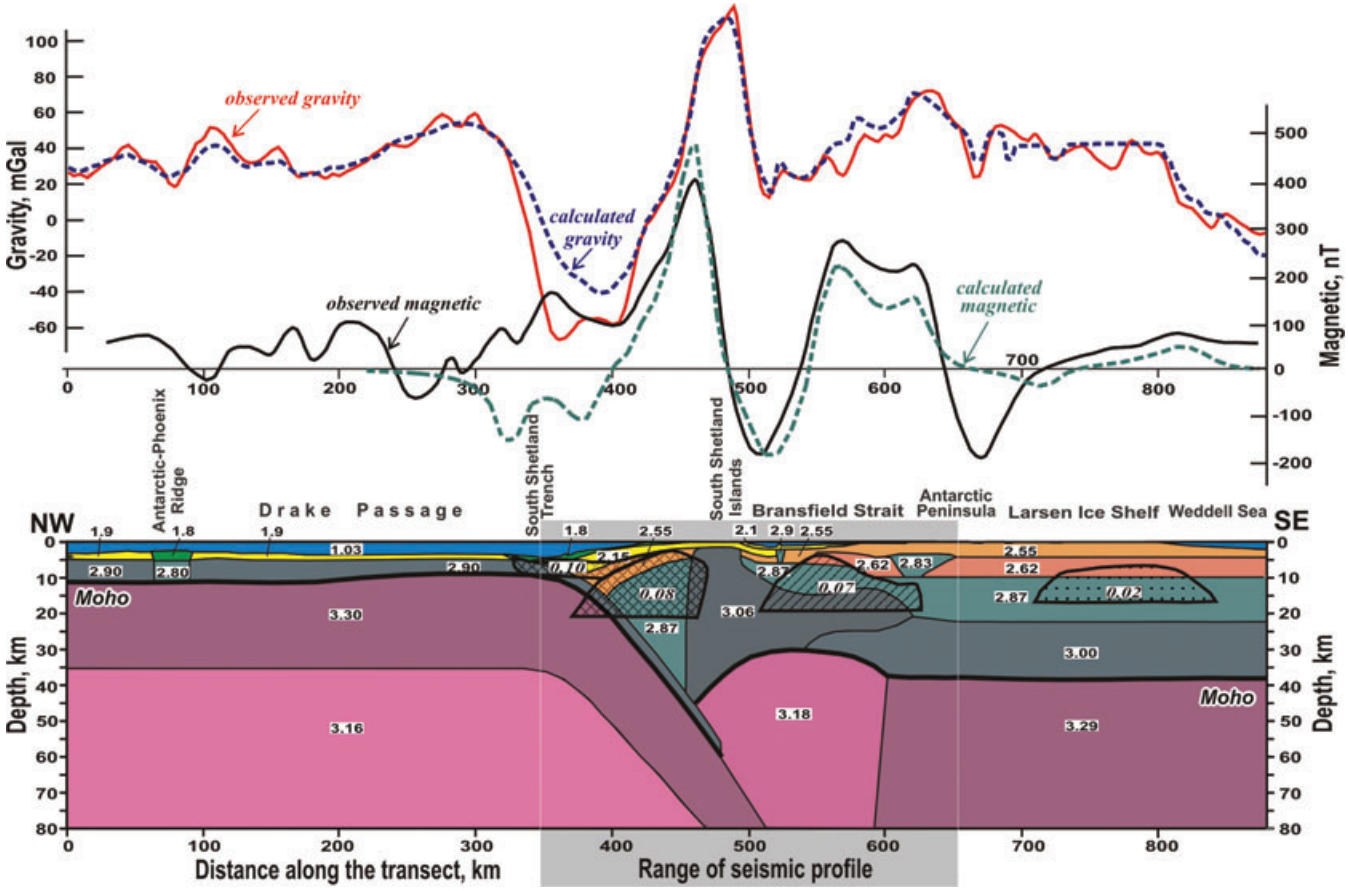

Figure 11. Density and magnetic model of the crust and upper mantle across Drake Passage and Bransfield Strait to the Antarctic Peninsula, line I-I (along the DSS-17 line). Location of lines is shown in Fig. 2. Observed and calculated anomalies are shown in the upper part of the figure. Numbers on the cross-section indicate density values in g cm^{-3}. Hatched domains above the 20-km-depth level shows magnetic bodies with calculated susceptibility (numbers in italic, SI units).

6.5 km s^{-1} velocity, which could be a layered intrusion of mafic rocks (gabbro).

Our gravity modelling shows strong density heterogeneities in the upper mantle. Continental crust of the AP is underlain by upper mantle of 3.29 g cm^{-3} density. In order to explain the gravity field above the Bransfield Strait and the presence of a high-velocity/density crustal body, a low-density (3.18 g cm^{-3}) uppermost mantle is assumed below the rift (Fig. 11). Since the density values in the uppermost mantle beneath the Bransfield rift depends on the presence of an anomalous crustal body, which is a well constrained feature of all seismic lines crossing the Bransfield rift, a series of calculations incorporating slight density variations in the crustal body were made. Calculations were made for a crustal body with an average density of 2.98, 3.0 and 3.05 g cm^{-3} and a constant upper mantle density below the rift was taken to be 3.25, 3.30 and 3.28 g cm^{-3} for each case, respectively. The calculated response for these models is systematically lower than the observed values and this is interpreted as supporting the occurrence of a low-density mantle beneath the rift zone. Fig. 11 shows the model with 3.18 g cm^{-3} density derived for the upper mantle below the Bransfield rift.

Upper mantle of the oceanic domain is characterized by high seismic velocities below the Moho and the presence of a seismic reflector. High seismic velocities below the subducting oceanic Moho are modelled as oceanic lithosphere of 3.30 g cm^{-3} density. Low velocity below seismic reflector was constrained by lower densities of 3.16 g cm^{-3} (Fig. 11).

8 DENSITY MODEL OF THE CRUST AND UPPER MANTLE FROM THE BELLINGSHAUSEN SEA TO THE ANTARCTIC PENINSULA

A second model was computed along the 520-km-long line II-II crossing the AP continental margin in the area of Anvers Island from the Bellingshausen Sea to Jason Peninsula (Fig. 2). It runs along the DSS-12 profile (Fig. 6a), which constitutes the central part of line II-II. This line crosses a strong (100 mGal) Free-Air gravity anomaly at the edge of the continental slope and the PMA consisting of two branches—western and eastern—of 300 and 250 nT, respectively (Figs 5 and 12). The final density model along the line II-II is shown in Fig. 12. The model has been fitted with 7 mGal of average deviation between the calculated and the observed field, which, taking into account the variation of Free-Air anomalies from −10 to 90 mGal, constitutes 7 per cent of the maximum amplitude of the gravity field along the line.

The density model in Fig. 12 shows two crustal blocks—oceanic and continental. The continental block, including the western shelf of the AP, the AP mainland and the Larsen Ice Shelf, has a 40-km thick crust with a 20-km-thick middle crust of 2.87 g cm^{-3} average

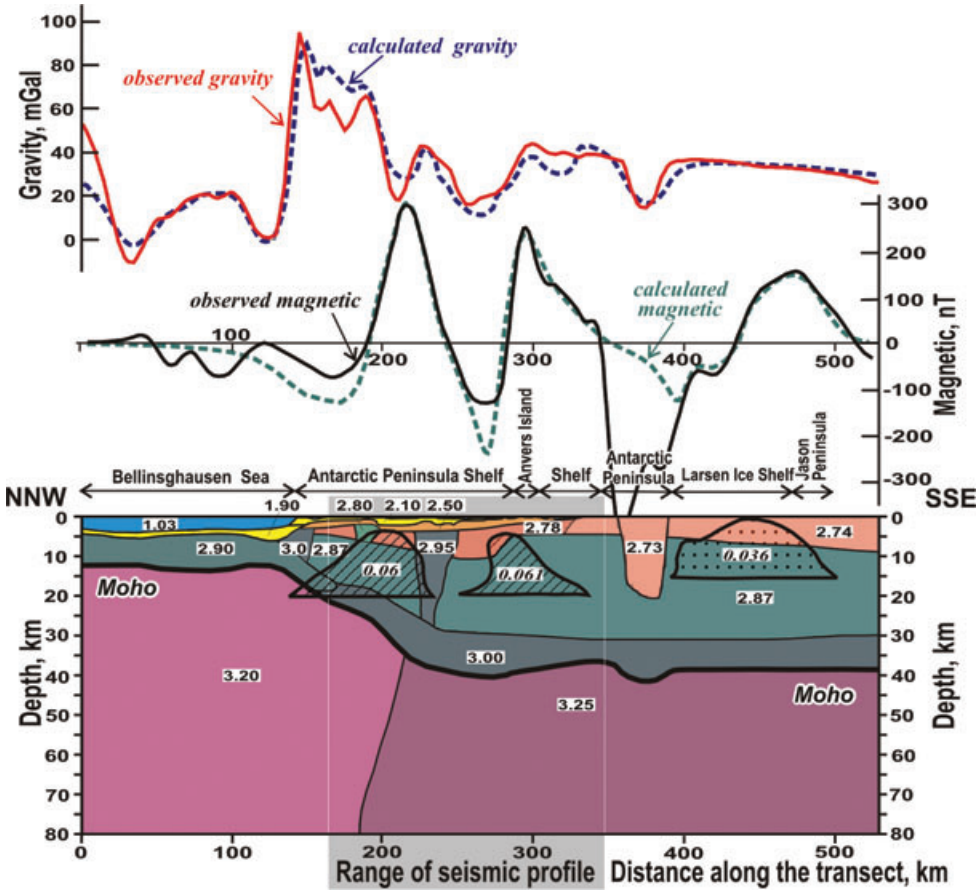

Figure 12. Density and magnetic model of the crust and upper mantle from the Bellinshausen Sea to the Antarctic Peninsula, line II-II. Location of lines is shown in Fig. 2. Observed and calculated anomalies are shown in the upper part of the figure. Numbers on the cross-section indicate density values in g cm^{-3}. Domains with hatching above the 20-km-depth level shows magnetic bodies with calculated susceptibility (numbers in italic, SI units).

density. High densities (∼3.0 g cm^{-3}) were obtained in the 10-km-thick lower crust. Thin upper crystalline crust is characterized by densities in the range of 2.74–2.78 g cm^{-3}. In the subsurface layer of the AP a basement is distinguished with $V_p = 5.11$ km s^{-1} and $\rho = 2.50$ g cm^{-3}, which is represented, most likely, by compacted sediments (metasediments) and intercalated volcanics.

Since the oceanic domain along the line II-II is not elucidated by the DSS-12 line, its geometry was taken from neighbouring seismic line DSS-17, the only profile crossing oceanic crust (Fig. 6). The oceanic crustal domain shows a 7-km-thick crystalline crust of 2.9 g cm^{-3} density overlain by thin (∼1 km) oceanic sediments of 1.9 g cm^{-3} density under the 3.5–4 km sea water column. The thickness of sediments in the Bellingshausen Sea was taken from a seismic reflection study (Scheuer *et al.* 2006).

Major changes in the crustal structure were determined in the transition block, where within a distance of 100 km the crust thickens from 10 to 25 km. It represents an uplifted crustal block of average density 2.87 g cm^{-3}, which is marked by a linear gravity high (Fig. 12). This uplifted block, in the form of a wedge, is very similar to that found along the line I-I in Fig. 11. Westwards from this high, one can see a gravity low that is caused by 3-km-thick sediments of a former accretionary wedge. Colocation of the uplifted dense crustal block with the magnetic body of 0.06 SI susceptibility that is interpreted to cause the western branch of the PMA (Fig. 12) is indicative of their common sources. Another magnetic body of the same susceptibility, determined in the area of Anvers Island, explains the eastern anomaly of the PMA. Derived values of the magnetic susceptibility and density indicate that these magnetic bodies, which are located in the upper 20 km layer, are mainly composed of mafic rocks (diorite, gabbro, and gabbro-diorite; see Table 1).

9 DISCUSSION

The main results derived from our potential field models are discussed here in terms of tectonic structures and tectonic processes that developed along the Pacific margin of the AP.

9.1 Active continental margin

On-going tectonic processes operate within the northern sector of the AP continental margin—in the area of South Shetland Trench—Bransfield Strait (profile I-I, Fig. 11), which is bounded by the Shackleton and Hero fracture zones. The presence of an active continental margin here is highlighted by belts of strong gravity and magnetic anomalies caused by subduction and recent continental rifting processes. Subduction is revealed in Fig. 11 by underthrusting of the oceanic lithospheric slab of Drake Passage (Phoenix Plate in Fig. 1) under the South Shetland Islands. The subducting slab represents a coupled oceanic crust ($\rho = 2.9$ g cm^{-3} and $V_p = 7.0$ km s^{-1}) and underlain lithosphere ($\rho = 3.3$ g cm^{-3} and $V_p = 8.3$ km s^{-1}) bound by a seismic reflector parallel to the Moho boundary. At present the subduction of the remnant of the Phoenix

Plate is assumed to be ongoing at low rates or it may have ceased (Galindo-Zaldivar *et al.* 2000; Maldonado *et al*. 2000). On-going subduction is consistent with observed seismicity, which shows that many earthquakes have focal mechanisms and depths (∼30 km) indicative of underthrusting of an oceanic slab below the South Shetland Trench/Islands system (Robertson *et al.* 2003; Pelayo & Wiens 1989).

9.1.1 South Shetland Trench

Due to subduction, an accretionary trough has been formed in the South Shetland Trench. It is filled with 5-km-thick accretionary sediments of 2.15 g cm^{-3} density (V_p = 4.2 km s^{-1}), overlain by thin oceanic sediments (density 1.8 g cm^{-3}). The sediments and the deep-water trench are largely responsible for a strong gravity low in the South Shetland Trench (Fig. 11). Landward progradation of the subduction front has, led to the formation of an uplifted crustal wedge of 2.87 g cm^{-3} density and high magnetic susceptibility (0.08 SI) that causes the strong gravity and magnetic anomalies. Strongly magnetized (susceptibility 0.1 SI) and thick formations of metasedimentary basement and intercalated volcanics also contribute to this magnetic anomaly. Thus, the combined effect of volcanic rocks and a large uplifted crustal wedge intruded by magmatic rocks of mafic composition (gabbro) provides a reasonable explanation for the strong magnetic anomaly of the western branch of the PMA in the South Shetland Trench region (Fig. 11).

9.1.2 South Shetland Islands

The archipelago of the South Shetland Islands, marked by a belt of strong gravity anomalies and a lack of corresponding magnetic anomalies, is caused by a large crustal batholith of ultrabasic rocks (peridotites) of 3.06 g cm^{-3} average density (Figs 11 and 13). The batholith was intruded into the crust as a result of partial melting in the uppermost mantle that occurred during Cretaceous subduction (González-Ferrán 1985; Leat *et al.* 1995). Alternatevely, the ultramafic batholith may relate to terrane accretion process that occurred further south along the palaeo-Pacific margin of the AP (Vaughan & Storey 2000; Ferraccioli *et al.* 2006). Mafic rocks of the AP batholith of predominantly early Cretaceous age (Leat *et al.* 1995) are the most widespread rocks exposed on the islands of the AP shelf and mainland (Table 1, Fig. 9). Exposures of ultramafic rocks (metadunites, serpentinites) were found on Gibbs Island, which is included in the group of northern islands of the archipelago of the South Shetland Islands (De Wit *et al.* 1977; Silant'ev *et al.* 1997) and is exposed at the southeastern end of the Shackleton fracture zone. Geochemical and petrological characteristics of these ultramafic rocks indicate that they originate from ultramafic cumulates, which were intruded, probably in the Early Cretaceous, from the upper mantle into a tectonic collage of composite magmatic arc complexes of the South Shetland Islands (Silant'ev *et al.* 1997).

9.1.3 Bransfield rift

Located between the South Shetland Islands and the AP, the Bransfield trough has typical features of a rift zone. It is an asymmetrical graben with a steep northwestern flank, on the South Shetland Islands side, and a wide, gently sloping southeastern flank, formed by the AP shelf. Sedimentary fill of the Bransfield Basin consists of a 1–4 km thick sequence of sediments of density 2.15–2.20 g cm^{-3}, which, in turn, cover metasedimentary basement rocks and intercalated volcanics (V_p = 5.4 km s^{-1} and ρ = 2.55 g cm^{-3}). These volcanic rocks occur in volcanic edifices and seamounts, which form a chain of neotectonic volcanoes along the Bransfield rift axis (Smellie 1988, 1989; Keller *et al.* 2002; Somoza *et al.* 2004).

The crystalline crust of the Bransfield rift is highly anomalous because of the occurrence of a 15-km-thick body in the mid-lower crust, with high-velocity (7.4–7.7 km s^{-1}) and density (3.06 g cm^{-3}). Bodies of this type have been recognized in several rifts and are attributed to a 'rift pillow' or mantle underplating (Ervin & McGinnis 1975; The DOBREfraction'99 Working Group 2003; Yegorova *et al.* 1999). By analogy we interpret the high velocity and high-density crustal body of the Bransfield rift as indicative of an extensive magmatic underplating during rifting. This has led to modification of the uppermost mantle and to substantial Moho uplift below the central part of the rift (up 30 km depth), that is 10 km shallower than the Moho position on the neighboring AP shelf.

Knowledge of the structure of the lower crust and upper mantle below the rift zones is important in order to understand rift-related magmatic processes. Well-studied rift zones of Kenya, Rio Grande and Rhine Graben also feature crustal thinning and significant amounts of magmatic underplating (Keller *et al.* 1991, 1994; Prodehl *et al.* 1992). Mohr (1989) argues that almost the entire crust in Afar is new igneous material. This magmatic process, which involves large volumes of magmas of mafic and ultramafic composition uprising to the base of the crust can cause phase modifications within the lower crust (e.g. mafic granulites to eclogites transition, i.e. Yegorova *et al.* 1999). Newly formed rocks have higher densities and sink into the upper mantle, thus significant crustal material is lost into the upper mantle. Many rifts also feature a low-velocity zone in the upper mantle, interpreted to be caused by partial melting (3–5 per cent) of basaltic magma rising from greater depth up to the Moho (Makris & Ginzburg 1987; Prodehl *et al.* 1992; Davis *et al.* 1993; Achauer *et al.* 1994). Though no low *P*-wave velocities were determined from our seismic refraction survey, an independent surface wave seismic tomography study (Vuan *et al.* 2005) revealed a low *S*-wave velocity upper mantle (soft lid) that extends down to depth of >70 km below the Bransfield rift. These data correspond well with low upper mantle densities revealed from our gravity modelling, high values of surface heat flow and ongoing volcanic activity along the rift axis. All these lines of evidence suggest that anomalously hot upper mantle underlies the Bransfield rift.

9.2 Passive continental margin

The model along line II-II is interpreted as revealing the lithospheric architecture of the passive continental margin that was superimposed along a palaeosubduction zone within the AP margin near Anvers Island (Fig. 12). Although the gravity and magnetic anomaly belts continue along the passive margin segment of the AP, their amplitudes are reduced compared to the active margin segment. Fig. 12 shows the crustal structure, which is typical for a passive continental margin, where the thin oceanic crust of the Bellingshausen Sea is juxtaposed against the thick continental crust of the AP. In the transition zone we imaged an uplifted crustal wedge intruded by mafic batholiths (Figs 12 and 13) that were probably emplaced during Cretaceous subduction (Leat *et al.* 1995). The Moho boundary deepens southeastwards and reaches a depth of 35 km below the AP shelf. The Moho relief is a consequence of palaeosubduction and underthrusting of the oceanic plate of the Bellingshausen Sea under the AP continental crust. Tectonic activity terminated here in Late Miocene–Early Pliocene because of the extinction of the Phoenix-Antarctic Ridge after the Phoenix Plate was consumed in

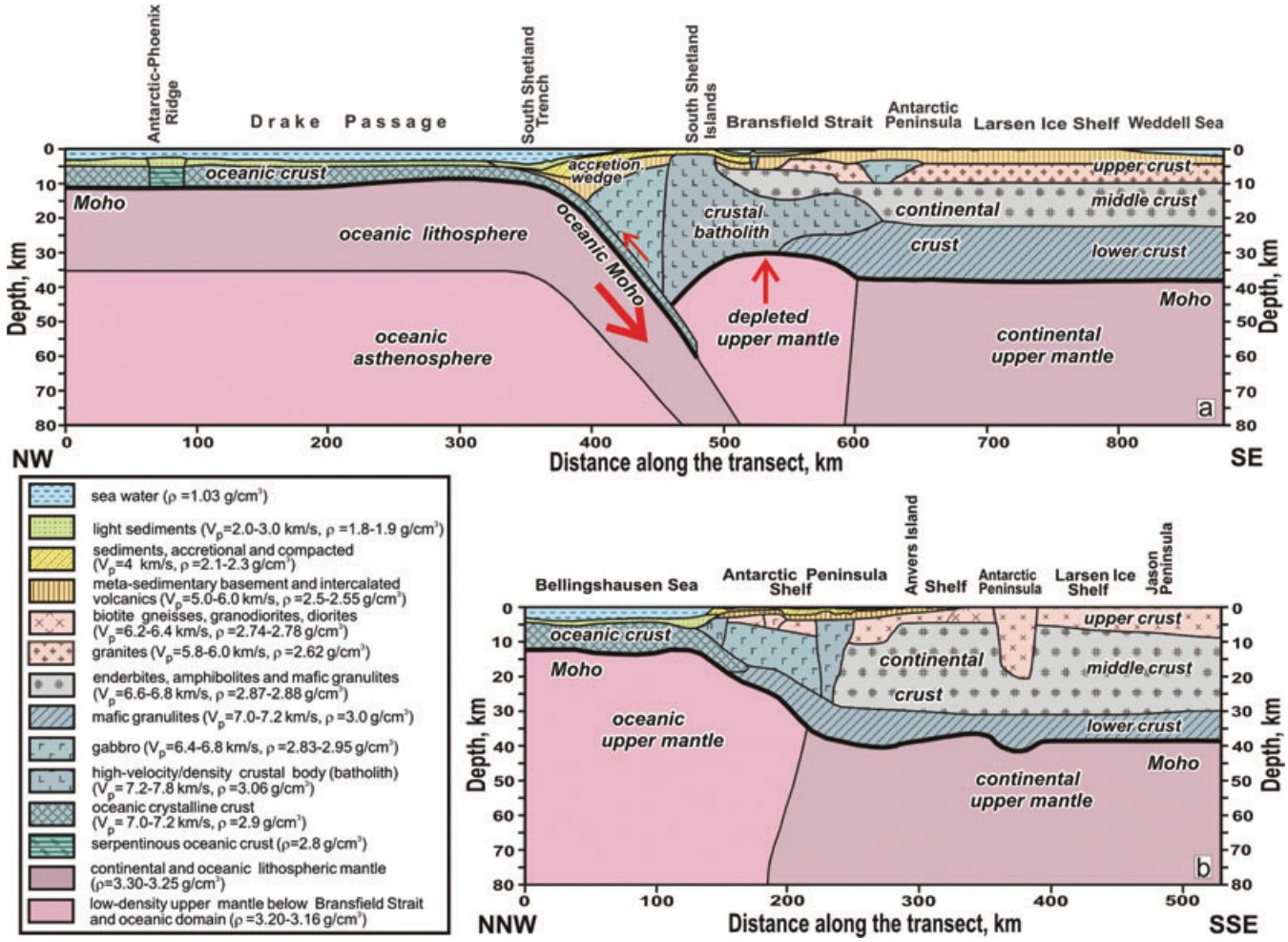

Figure 13. Petrological models for the crust and upper mantle for active (a, section I-I) and passive (b, section II-II) types of the Antarctic Peninsula continental margin. Compiled from the seismic models in Fig. 7, gravity and magnetic sections in Figs 11 and 12, and physical properties of main rock types and crustal layers (Figs 9, 10, Tables 1 and 2).

the subduction zone (Larter & Barker 1991; Galindo-Zaldivar *et al.* 2000; Maldonado *et al.* 2000; Eagles *et al.* 2009).

9.3 Transition from passive to active continental margin

The Drake Passage is separated in the southwest, from the Bellingshausen Sea, by the Hero fracture zone and to the northeast—by the Shackleton fracture zone, separating the Drake Passage from the Scotia Sea. Consequently, a boundary between active (line I-I) and passive (line II-II) continental margin styles in the AP should occur in the area of the Hero fracture zone (Fig. 1). Though no direct indication of recent tectonic activity (e.g. recorded seismicity or strike-slip faulting) is observed here, the Hero fracture zone is considered to be a prominent crustal structural discontinuity.

In particular, the Hero fracture zone is clearly identified from elongated Free-Air anomaly highs of 100–150 mGal amplitude (Fig. 4) flanked by gravity lows. In addition, the Hero fracture zone represents a step-like fault on the sea floor, which divides the Drake Passage Plate with 3500–3700 m bathymetry from the deeper part (4100–4300 m) of the Bellingshausen Sea (Fig. 2). Multichannel seismic studies conducted at the SW end of South Shetland Trench show evidence in the Hero fracture zone of the transition from an active to a passive margin (Jabaloy *et al.* 2003). A 1000-km-long combined seismic section, constructed by Grad *et al.* (2002) along the AP margin between Marguerite Bay and Elephant Island, shows a major crustal boundary, which corresponds to the southeastward projection of the Hero fracture zone. This discontinuity separates a thick (about 40 km) three-layer continental crust of the AP to the southwest from thinner two-layer crust with high-velocity intrusions that extends beneath the Bransfield Strait to the northeast.

9.4 Composition of the crustal blocks (petrological model)

The obtained distribution of physical parameters (density, magnetic susceptibility and *P*-wave seismic velocity) permits conclusions to be drawn about the composition of the main blocks and crustal layers (Fig. 10 and Table 2). In addition, it is possible to infer the composition of the upper crust and intrusive complexes by using both the petrology and physical properties of the rock complexes (Table 1 and Fig. 9). For deeper levels a global study on seismic structure and composition of the continental crust (Christensen & Mooney 1995) was used. The inferred petrological model for the sections I-I and II-II is shown in Fig. 13.

The AP features 38–40-km-thick continental crust. Three-layers are recognized here. The 10-km-thick upper crust with V_p = 6.0–6.45 km s^{-1} and ρ = 2.62–2.77 g cm^{-3} is assumed to be composed of granites, granodiorites, diorites and biotite (tonalite) gneisses (see also Tables 1 and 2, Figs 9 and 10). The middle crust of V_p = 6.5–6.8 km s^{-1} and average ρ = 2.87 g cm^{-3} occurring down to a depth of 23–29 km, is represented mostly by enderbites and, to a lesser extent, by amphibolites and mafic granulites. Mafic granulites prevail in the lower crust (V_p = 7.0–7.2 km s^{-1} and $\rho \sim$ 3.0 g cm^{-3}) and are replaced in the lowermost crust (above the Moho) by garnet mafic granulites (Fig. 13). This type of crust links the AP crust to continental arc crust rather than to shields and platforms (Christensen & Mooney 1995). According to this classification, both crust types are very similar and are characterized by the presence of 10-km-thick high-velocity lower crust, though velocities in the upper crust of the continental arcs crust are higher than that in the crust of shields and platforms. The presence of a high-velocity and density lower crust beneath the AP could be caused by alteration of the continental crust during the formation of a magmatic arc.

The two-layered crust of the Bransfield Strait is defined by much higher velocities and densities and also by a shallower Moho than that determined by Christensen & Mooney (1995) for the average section of rifts. Fig. 13 shows that the upper crust below the Bransfield Rift (V_p = 5.5–6.9 km s^{-1}, ρ = 2.85 g cm^{-3} and æ = 0.07 SI) is represented by gabbro, gabbro-norites and gabbro-anorthosites. The lower crust (V_p = 7.2–7.7 km s^{-1} and ρ = 3.05 g cm^{-3}) is assumed to be composed of ultramafic rocks (peridotites) and mafic rocks (gabbro-norites), which form a high-velocity body related to widespread mantle underplating (Fig. 13).

9.5 Variation of the uppermost mantle density

Our gravity modelling indicates density variations in the uppermost mantle within the study region. The continental crust of the AP is underlain by upper mantle of 3.29–3.25 g cm^{-3} density and 8.10 km s^{-1} velocity, which is considered to be normal for Precambrian and Phanerozoic platforms.

The anomalous upper mantle of 3.18 g cm^{-3} density below the Bransfield Strait and South Shetland Islands is indicative of temperature mobilization of the upper mantle below the rift zone and modification of the uppermost mantle due to melting of large volumes of magma that were intruded into the lower crust (depleted upper mantle in Fig. 13a). The occurrence of soft mantle at a shallow depth could give rise to high values of surface heat flow reaching 250 mW m^{-2} in the central part of the basin (Lawver & Nagihara 1991; Lawver *et al.* 1995) and strong hydrothermal activity (Suess *et al.* 1987; Schloesser *et al.* 1988; Dählmann *et al.* 2001; Klinkhammer *et al.* 2001; Somoza *et al.* 2004). Surface wave seismic tomography performed for the area of Bransfield Strait by joint inversion of Rayleigh and Love dispersion curves from 15 to 50 s reveals that low upper mantle velocities (soft lid) extend down to depths exceeding 70 km (Vuan *et al.* 2005). This low velocity upper mantle below the Bransfield Strait is explained by Vuan *et al.* (2005) by elevated temperatures and may indicate a mantle plume or asthenospheric diapir.

Oceanic crust of the Drake Passage is underlain by high-velocity (8.3 km s^{-1}) and high-density (3.3 g cm^{-3}) upper mantle assuming unaltered lithospheric mantle. The best candidates for composition of the lithospheric mantle in the Drake Passage are dunites. The lithospheric mantle occurs down to a depth of 35 km, where it is confined by a seismic reflector. The relief of this reflector conforms to the topography of the underthrusting Moho (Figs 7a and 13a) and delineates the Phoenix Plate subducting beneath the South Shetland Trench. We interpret this seismic boundary in the lower oceanic lithosphere to be of thermal origin (however, it could be also compositional) by analogy with the subduction zone in continental Chile, where approximately at these depths the 700 °C isotherm was estimated by Contreras-Reyes *et al.* (2008). In this case the presence of a soft upper mantle with density 3.16 g cm^{-3} for the depth deeper than 35 km may be indicative of a shallow asthenosphere (Figs 11 and 13a).

9.6 Comparison of the subduction zone below the South Shetland Islands with other subduction zones

Gravity and magnetic anomalies are prominent features of subduction zones and magmatic arcs worldwide (Grow & Bowin 1975; Finn 1994; Clowes & Hyndman 2002; Blakely *et al.* 2005). Belts of gravity anomalies consisting of gravity lows and highs are developed along the active continental margins: gravity lows are caused by water and sediments in the deep sea trench, whereas gravity highs are developed over the descending slab and are assumed to be caused by modification of the crust and uppermost mantle by subduction (Lowrie 1997).

In this regard it is useful to make a comparison of our modelling results along the subduction zone of South Shetland Islands (line I-I) with the northern Cascadia subduction zone (Clowes & Hyndman 2002) and the subduction zone below continental Chile (Grow & Bowin 1975; Contreras-Reyes *et al.* 2008). The principal structural elements of these subduction zones are: the underthrusting oceanic plate and the overlying accretionary sedimentary wedge. The subducting oceanic slab consists of coupled thin (6–7 km) oceanic crust (V_p = 6.8–7.3 km s^{-1} and $\rho \sim$ 2.9 g cm^{-3}) and mantle lithosphere (V_p = 8.2–8.3 km s^{-1}, $\rho \sim$ 3.3 g cm^{-3}; Clowes & Hyndman 2002; Contreras-Reyes *et al.* 2008). High-velocity uppermost mantle in the Chile subduction zone (below the Moho) was explained by Contreras-Reyes *et al.* (2008) by inferring the presence of eclogitic rocks. However, the average V_p = 8.0 km s^{-1} of these rocks and the extremely high density (about 3.5 g cm^{-3}, Christensen & Mooney 1995), which are much higher than that derived for the oceanic lithosphere in Figs 11 and 13, are not adequate to explain the eclogite composition of the AP active continental margin. Dunits match better to obtained velocity and density values in oceanic lithosphere of Drake Passage. The structure of the subducting lithospheric slab and underlying oceanic asthenosphere of the northern Cascadia subduction zone (Clowes *et al.* 1999; Clowes & Hyndman 2002) is very similar to that below the South Shetland Trench and Islands (Figs 7a, 11 and 13).

An important feature of the continental crust in the region of northern Cascadia subduction zone is a high-velocity/density block in the lower crust causing a 50-mGal gravity high, which is explained by remnants of the older, underthrusted, oceanic plate accreted along the margin (Clowes & Hyndman 2002). In this regard it has some similarities with high-velocity/density crustal body of the South Shetland Islands, responsible for a 100-mGal gravity high, caused by huge batholith of mantle cumulates intruded into the crust during Cretaceous subduction. The backarc basin of the Bransfield Strait is an extra element of the active segment of the AP continental margin, which is absent in the region of subduction zones of northern Cascadia and below continental Chile. This stage relates to ongoing continental rifting on the margin of the AP, which manifests itself in strong magmatic and volcanic activity.

10 CONCLUSIONS

The continental margin of the AP provides a unique opportunity to study the deep structure of continental margins and magmatic arcs since it is covered by a dense network of deep seismic refraction profiles and features strong gravity and magnetic anomalies associated with AP batholith. We investigated the lithosphere structure of the AP by combining deep seismic refraction studies with magnetic and gravity modelling. 2-D gravity and magnetic modelling, carried out along two interpretation lines parallel to seismic profiles (DSS-17 and DSS-12), yielded models of the crust and upper mantle structure. In addition, we proposed a new petrological model for the margin and revealed a heterogeneous structure in the upper mantle. The joint analysis of seismic velocities and potential field signatures allowed us to draw the following conclusions:

(1) The active margin segment of the northern AP is characterized by ongoing subduction beneath the South Shetlanf Trench and active continental rifting in the Bransfield Strait. A good image of the 35-km-thick oceanic plate, consisting of thin oceanic crystalline crust and lithospheric mantle subducting below the South Shetland Islands, is shown in Figs 7(a), 11 and 13. Subduction resulted in the deep-water South Shetland Trench and accretionary sediments of 8 km total thickness, which result in a stripe gravity low of −60 mGal. Belts of strong gravity and magnetic anomalies along the AP are caused by large mafic plutons linked to partial melting in the upper mantle and lower crust and associated with Cretaceous subduction. Our modelling shows that the South Shetland Islands represent the exposed part of a huge crustal diapir, which is composed mostly of Cretaceous ultramafic rocks (peridotites).

(2) The passive margin segment of the northern AP is characterized by juxtaposition of thin oceanic crust of the Bellingshausen Sea and *ca*. 40-km-thick continental crust of the AP. The transition zone includes an uplifted crustal wedge that is interpreted by mafic intrusions assigned to the AP batholith.

(3) Our model of the Bransfield Rift supports its origin as a continental back arc basin that has been significantly affected by continental rifting processes. The rift features significant crustal thinning and the presence of a high-velocity and high-density body in the crust that is interpreted as reflecting widespread underplating. Additionally, we interpret ongoing tectonic and magmatic activity within the Bransfield Strait as related to mobilization of warm, low-density upper mantle at shallow depth.

ACKNOWLEDGMENTS

The authors thank two anonymous reviewers for their valuable suggestions which improved paper.

REFERENCES

Achauer, U. & the KRISP Teleseismic Working Group, 1994. New ideas on the Kenya rift based on the inversion of the combined dataset of the 1985 and 1989–90 seismic tomography experiments, *Tectonophysics,* **236,** 305–329.

Artemenko, G.V., Bakhmutov, V.G., Gladkochub, D.S. & Samborskaya, I.A., 2009. Geochemistry and ore-bearing of intrusion basites of the Antarctic Peninsula, in *Abstracts of IV International Antarctic Conference 'III International Polar Year 2007–2008: Results and Outlooks',* pp. 28–31, Ministry of Education and Science of Ukraine, Kiev.

Ashcroft, W.A., 1972. Crustal structure of the South Shetland Islands and the Bransfield Strait, *Br. Antarct. Surv. Sci. Rep.,* **66,** 43.

Baker, P.E., Davies, T.G. & Roobol, M.J., 1969. Volcanic activity at Deception Island in 1967 and 1968, *Nature,* **224,** 553–560.

Barker, P.F., 1982. The Cenozoic subduction history of the Pacific margin of the Antarctic Peninsula: ridge–crest interactions, *J. geol. Soc. Lond.,* **139,** 787–801.

Barker, D.H.N., Christeson, G.L., Austin, J.A. & Dalziel, I.W.D., 2003. Backarc basin evolution and Cordilleran orogenesis: insights from new ocean-bottom seismograph refraction profiling in Bransfield Strait, Antarctica, *Geology,* **31,** 107–110.

Birch, F., 1960. The velocity of compressional waves in rocks to 10 kilobars. Pt. 1, *J. geophys. Res.,* **65**(4), 1083–1102.

Birch, F., 1961. The velocity of compressional waves in rocks to 10 kilobars. Pt. 2, *J. geophys. Res.,* **66**(7), 2199–2224.

Birkenmajer, K., 1987. Report on the Polish geological investigations in the Antarctic Peninsula sector, West Antarctica, in 1984–1985, *Stud. Geol. Pol.,* **43,** 11–122.

Blakely, R.J., Brocher, T.M. & Wells, R.E., 2005. Subduction zone magnetic anomalies and implications for hydrated forearc mantle, *Geology,* **33**(6), 445–448.

Christeson, G.L., Barker, D.H.N., Austin, J.A. & Dalziel, W.D., 2003. Deep structure of Bransfield Strait: initiation of a back arc basin by rift reactivation and propagation, *J. geophys. Res.,* **108,** 2492, doi:10.1029/2003JB002468.

Christensen, N.I. & Mooney, W., 1995. Seismic velocity structure and composition of the continental crust: a global view, *J. geophys. Res.,* **100,** 9761–9788.

Clowes, R.M. & Hyndman, R.D., 2002. Geophysical studies of the northern Cascadia subduction zone off western Canada and their implications for great earthquake seismitectonics: a review, in *Seismotectonics in Convergent Plate Boundary,* pp. 1–23, eds Fujinawa, Y. & Yoshida, A., Terra Scientific Publishing Company, Tokyo.

Clowes, R.M.F., Cook, F.A., Hajnal, Z., Hall, J., Lewry, J., Lucas, S. & Waerdle, R., 1999. Canada's Lithoprobe Project (collaborative, multidisciolinary geoscience research leads to new understanding of continental evolution, *Episodes,* **22,** 3–20.

Contreras-Reyes, E., Grevemeyer, I., Flueh, E.R. & Reichert, C., 2008. Upper lithospheric structure of the subduction zone offshore of southern Arauco peninsula, Chile, at ∼38° S, *J. geophys. Res.,* **113,** B07303, doi:10.1029/2007JB005569.2008.

Cooper, G.R.J., 1997. Forward modelling of magnetic data, *Comput. Geosci.,* **23**(10), 1125–1129.

Dählmann, A., Wallmann, K., Sahling, H., Sartou, G., Borhmann, G., Petersen, S., Chin, C.S. & Klinkhammer, G.P., 2001. Hot vents in ice-cold ocean: indications for phase separation at the southernmost area of hydrothermal activity, Bransfield Strait, Antarctica, *Earth planet. Sci. Lett.,* **193,** 381–394.

Dalziel, I.W.D. & Elliot, D.H., 1982. West Antarctica: problem child of Gondwanaland, *Tectonics,* **1,** 3–19.

Davey, F.J., 1972. Marine gravity measurements in the Bransfield Strait adjacent areas, in *Antarctic Geology and Geophysics,* pp. 39–46, ed. Adie, R.J., Universitetsforl., Oslo.

Davis, P. *et al*., 1993. Teleseismic tomography of continental rift zones, in *Seismic Tomography: Theory and Practice,* pp. 397–439, eds Iyer, H.M. & Hirahara, K., Chapman and Hall, London.

De Wit, M.J. *et al*., 1977. Deformation, serpentinization and emplacement of a dunite complex, Gibbs Island, south Shetland Islands: possible fracture zone tectonics, *J. Geol.,* **85**(6), 745–762.

DOBREfraction'99 Working Group, 2003. DOBREFraction'99—velocity model of the crust and upper mantle beneath the Donbas Foldbelt (East Ukraine), *Tectonophysics,* **371,** 81–110.

Eagles, G., Gohl, K. & Larter, R.D., 2009. Animated tectonic reconstruction of the southern Pacific alkaline volcanism at its convergent margins since Eocene times, *Tectonophysics,* **464,** 21–29.

Ervin, C.P. & McGinnis, L.D., 1975. Reelfoot rift: reactivated precursor to the Mississippi Embayment, *Geol. Soc. Am. Bull.,* **86,** 1287–1295.

Ferraccioli, F., Jones, P.C., Vaughan, A.P. & Leat, P.T., 2006. New aerogeophysical view of the Antarctic Peninsula: more pieces, less puzzle, *Geophys. Res. Lett.,* **33,** doi:10.1029/2005GL024636.

Ferraccioli, F., Jones, P.C., Leat P. & Jordan, T.A., 2007. Airborn geophysics as a tool for geoscientific research in Antarctica: some recent examples, in *Antarctica: A Keystone in a Changing Word – Omline Proceedings of the 10th ISAES,* eds Cooper, A.K., Raymond, C.R. *et al*., USGS Open-File Report 2007–1047, Short research Paper 056, 4 p., doi:10.3133/of2007–1047.srp056.

Finn, C., 1994. Aeromagnetic evidence for a buried Early Cretaceous magmatic arc, northeast Japan, *J. geophys. Res.,* **99,** 22 165–22 185.

Fretzdorff, S., Worthington, T.J., Haase, K.M., Hékinian, R., Franz, L., Keller, R.A. & Stoffers, P., 2004. Magmatism in the Bransfield Basin: rifting of the South Shetland Arc?, *J. geophys. Res.,* **109,** B12208, doi:10.1029/2004JB003046.

Galindo-Zaldivar, J., Jabaloy, A., Maldonado, A. & Galdeano, C., 1996. Continental fragmentation along the South Scotia Ridge transcurrent plate boundary (NE Antarctic Peninsula), *Tectonophysics,* **258,** 275–301.

Galindo-Zaldivar, J., Jabaloy, A., Maldonado, A., Martinez-Martinez, J.M., Galdeano, C.S., Somoza, L. & Surinach, E., 2000. Deep crustal structure of the area of intersection between the Shackleton Fracture Zone and the West Scotia Ridge (Drake Passage, Antarctica), *Tectonophysics,* **320,** 123–139.

Galindo-Zaldivar, J., Gambo, L., Maldonado, A., Nakao, S. & Bochu, Y., 2004. Tectonic development of the Bransfield Basin and its prolongation to the South Scotia Ridge, northern Antarctic Peninsula, *Mar. Geol.,* **6,** 267–282.

Garrett, S.W., 1990. Interpretation of reconnaissance gravity and aeromagnetic surveys of the Antarctic Peninsula, *J. geophys. Res.,* **95,** 6759–6777.

Garrett, S.W. & Storey, B.C., 1987. Lithospheric extension on the Antarctic Peninsula during Cenozoic subduction, in *Continental Extensional Tectonics,* Vol. 28, pp. 419–432, eds Coward, M.P., Dewey, J.F. & Hancock, P.L., Geol. Soc. London Spec. Publ.

Goldring, D.C., 1962. The geology of the Loubet Coast, Graham Land, *Br. Antarct. Surv. Sci. Rep.,* **36,** 50.

Golynsky, A.M. *et al*., 2001. *ADMAP – Magnetic anomaly map of the Antarctic, 1:10 000 000 scale map*, BAS (Misc) 10.

González-Casado, J.M., Gincr-Robles, J.L. & López-Martínez, J., 2000. Bransfield Basin, Antarctic Peninsula: not a normal back-arc basin, *Geology,* **28,** 1043–1046.

González-Ferrán, O., 1985. Volcanic and tectonic evolution of the northern Antarctic Peninsula: Late Cenozoic to recent, *Tectonophysics,* **114,** 389–409.

Gràcia, E., Canals, M., Farràn, M., Prieto, M.J., Sorribas, J. & GEBRA Team, 1996. Morpho-structure and evolution of the Central and Eastern the Bransfield (NW Antarctic Peninsula), *Mar. geophys. Res.,* **18,** 429–448.

Grad, M., Guterch, A. & Środa, P. 1992. Upper crustal structure of Deception Island, the Bransfield Strait, West Antarctica, *Antarct. Sci.,* **1,** 460–476.

Grad, M., Guterch, A. & Janik T., 1993a. Seismic structure of the lithosphere across the zone of subducted Drake plate under the Antarctic plate, West Antarctica, *Geophys. J. Int.,* **115,** 586–600.

Grad, M., Guterch, A., Janik, T. & Środa, P., 1993b. 2-D seismic models of the lithosphere in the area of the Bransfield Strait, West Antarctica, *Polish Polar Res.,* **14,** 2, 123–151.

Grad, M., Shiobara, H., Janik, T., Guterch, A. & Shimamura, H., 1997. New seismic crustal model of the Bransfield Rift, West Antarctica from OBS refraction and wide-angle reflection data, *Geophys. J. Int.,* **130,** 506–518.

Grad, M., Guterch, A., Janik, T. & Środa, P, 2002. Seismic characteristic of the crust in the transition zone from Pacific Ocean to the northern Antarctic Peninsula, West Antarctica, in *Antarctica at the Close of a Millennium,* **Vol. 35**, pp. 493–498, eds Gamble, J.A., Skinner, D.N.B. & Henrys, S., Royal Society of New Zealand Bulletin.

Grikurov, G.E., 1973. *Geology of the Antarctic Peninsula,* Nauka, Moscow (in Russian).

Grow, J.A. & Bowin, C.O., 1975. Evidence for high-density crust and mantle beneath the Chile Trench due to descending lithosphere, *J. geophys. Res.,* **80,** 1449–1458.

Guterch, A., Grad, M., Janik, T. & Środa, P., 1998. Polish Geodynamic Expeditions: seismic structure of West Antarctica, *Polish Polar Res.,* **19,** 1–2, 113–123.

Jabaloy, A. *et al*., 2003. The transition from an active to a passive margin (SW end of the South Shetland Trench, Antarctic Peninsula), *Tectonophysics,* **366,** 55–81.

Janik, T., 1997a. Seismic crustal structure in the transition zone between Antarctic Peninsula and South Shetland Islands, in *The Antarctic Region Geological Evolution and Processes,* pp. 679–684, ed. Ricci, C.A., *Proceedings of the VII International Symposium on Antarctic Earth Sciences, 10–15 September 1995, Siena (Italy),* Terra Antarctica Publication, Siena.

Janik, T., 1997b. Seismic crustal structure of the Bransfield Strait, West Antarctica. *Polish Polar Res.,* **18,** 3–4, 171–225.

Janik, T., Środa, P., Grad, M. & Guterch, A., 2006. Moho depths along the Antarctic Peninsula and crustal structure across the landward projection of the Hero fracture zone, in *Antarctica: Contributions to Global Earth Sciences,* pp. 229–236, eds Fütterer, D.K., Damaske, D., Kleinschmiddt, G., Miller, H. & Tessensohn, F., Springer-Verlag, Berlin, Heidelberg, New York.

Jin, Y.K., Larter, R.D., Kim, Y., Nam, S.H. & Kim, K.J., 2002. Post-subduction margin structures along Boyd Strait, Antarctic Peninsula, *Tectonophysics,* **346**(3–4), 187–200.

Johnson, A.C., 1996. Arc evolution: a magnetic perspective from the Antarctic Peninsula, *Geol. Mag.,* **133,** 637–644.

Johnson, A.C., 1999. Interpretation of new aeromagnetic anomaly data from central Antarctic Peninsula, *J. geophys. Res.,* **104,** 5031–5046.

Johnson, A.C. & Swain, C.J., 1995. Further evidence of fracture-zone induced tectonic segmentation of the Antarctic Peninsula from detailed aeromagnetic anomalies, *Geophys. Res. Lett.,* **22,** 1917–1920.

Jokat, W., Boebel, T., Konig, M. & Meyer, U., 2003. Timing and geometry of early Gondwana breakup, *J. geophys. Res.,* **108,** doi:10.1029/2002JB0011802.

Keller, G.R. *et al*., 1991. A comparative study of the Rio Grande and Kenya rifts, *Tectonophysics,* **197,** 355–372.

Keller, G.R. *et al*., 1994. The East African rift system in the light of KRISP 90, *Tectonophysics,* **236,** 465–483.

Keller, R.A., Fisk, M.R., Smellie, J.L., Strelin, J.A., Lawver, L.A. & White, W.M., 2002. Geochemistry of back arc basin volcanism in Bransfield Strait, Antarctica: subducted contributions and along-axis variations, *J. geophys. Res.,* **107,** doi:10.1029/2001JB000444.

Kim, Y., Choung, T.W. & Nam, S.H., 1992. Marine magnetic anomalies in the Bransfield Strait, Antarctica, in *Recent Progress in Antarctic Science. Proceedings of Sixth International Symposium on Antarctic Sciences, 9–13 September 1991, Tokyo,* pp. 431–437, eds Yoshda, Y. *et al*. Terra Scientific Publishing Company, Tokyo.

Kim, H.R., von Frese, R.R.B., Kim, J.W., Taylor, P.T. & Neubert, T., 2002. Ørsted verifies regional magnetic anomalies of the Antarctic lithosphere, *Geophys. Res. Lett.,* **29**(15), 8002, doi:10.1029/2001GL013662.

Kim, H.R., von Frese, R.R.B., Golynsky, A.V., Gaya-Pigue, L.R. & Ferraccioli, F., 2007. Improved magnetic anomalies of the Antarctic lithosphere, *Geophys. J. Int.,* **171,** 119–126.

Klepeis, K.A. & Lawver, L.A., 1996. Tectonics of the Antarctic-Scotia plate boundary near Elephant and Clarence Islands, West Antarctica, *J. geophys. Res.,* **101,** 20 211–20 231.

Klinkhammer, G.P. *et al*., 2001. Discovery of new hydrothermal vent sites in Bransfield Strait, Antarctica, *Earth planet. Sci. Lett.,* **193,** 395–407.

Larter, R.D. & Barker, P.F., 1988. The death throes of the Antarctic-Phoenix spreading system, *Geophys. J. Int.,* **92**(3), 553–553.

Larter, R.D. & Barker, P.F., 1991. Effects of ridge crest trench interaction on Antarctic-Phoenix spreading: forces on a young subducting plate, *J. geophys. Res.,* **96,** 19 583–19 607.

Larter, R.D., Cunningham, A.P., Barker, P.F., Gohl, K. & Nitsche, F.P., 2002. Tectonic evolution of the Pacific margin of Antarctica 1. Late Cretaceous tectonic reconstructions, *J. geophys. Res.,* **107**(B12), 2345, doi:10.1029/2000JB000052.

Lawver, L.A. & Nagihara, S., 1991. Heat flow measurements in the King George, the Bransfield Strait, in *Proceedings of Sixth International Symposium on Antarctic Sciences, 9–13 September 1991, Tokyo,* pp. 345, eds Yoshda, Y. *et al*. Terra Scientific Publishing Company, Tokyo.

Lawver, L.A., Keller, R.A., Fisk, M.R. & Strelin, J., 1995. The Bransfield Strait, Antarctic Peninsula: active extension behind a dead arc, in *Back-arc*

Basins, Tectonics and Magmatism, pp. 315–342, ed. Taylor, B., Plenum Publ. Corp., New York.

Leat, P.T., Scarrow, J.H. & Millar, I.L., 1995. On the Antarctic Peninsula batholith, *Geol. Mag.,* **132**(4), 399–412.

Lebedev, T.S., Shepel, S.I., Korchin, V.A., Burtnyi, P.A., Savenko, B.Ya., Shapoval, V.I. & Karnaukhova, E.E., 2002. Petrophysical characteristics of rocks of Antarctic Peninsula west cost and adjoining islands in the area of 'Akademic Vernadsky' station, *Geophys. J.,* **24,** 93–115 (in Russian).

Lowrie, W., 1997. *Fundamentals of Geophysics,* Cambridge University Press, 354 p.

Majdański, M., Środa, P., Malinowski, M., Czuba, W., Grad, M., Guterch, A. & Hegedűs, E., 2008. 3D seismic model of the uppermost crust of the Admiralty Bay area, King George Island, West Antarctica, *Polish Polar Res.,* **29**(4), 311–316.

Makris, J. & Ginzburg, A., 1987. The Afar Depression: transition between continental rifting and sea-floor spreading, *Tectonophysics,* **141,** 199–214.

Maldonado, A. *et al*., 2000. Tectonics of an extinct ridge-transform intersection, Drake Passage (Antarctica), *Mar. geophys. Res.,* **21,** 43–68.

Maslanyj, M.P., Garrett, S.W., Johnson, A.C., Renner, R.G.B. & Smith, A.M., 1991. Aeromagnetic anomaly map of West Antarctica, *BAS GEOMAP Series, Geophysical Map and Supplementary Text,* British Antarctic Survey, Cambridge, p. 37.

McAdoo, D. & Laxon, S., 1997. Antarctic tectonics: constraints from ERS-1 satellite marine gravity field, *Science,* **276,** 556–560.

Mohr, P., 1989. The nature of the crust under Afar: new igneous, not stretched continental, *Tectonophysics,* **167,** 1–11.

Nafe, J.E. & Drake, Ch.L., 1963. Physical properties of marine sediments, in *The Sea,* Vol. 3, pp. 794–815, ed. Hill, M.N., Interscience, New York.

Pelayo, A.M. & Wiens, D.A., 1989. Seismotectonics and relative plate motions in the Scotia Sea Region, *J. geophys. Res.,* **94,** 7293–7320.

Prodehl, C., Mueller, St., Glahn, A., Gutscher, M. & Haak, V., 1992. Lithospheric cross-sectinsof the European Central rift system, *Tectonophysics,* **208,** 113–138.

Renner, R.G.B., 1980. Gravity and magnetic surveys in Graham Land, *Brit. Antarct. Surv. Sci. Rep.,* **77,** 99.

Renner, R.G.B., Dikstra, B.J. & Martin, J.L., 1982. Aeromagnetic surveys over the Antarctic Peninsula, in *Antarctic Geoscience,* pp. 363–367, ed. Craddock, C., University of Wisconsin Press, Madison.

Renner, R.G.B., Sturgeon, L.J.S. & Garrett, S.W., 1985. Reconnaissance gravity and aeromagnetic surveys of the Antarctic Peninsul, *Brit. Antarct. Surv. Sci. Rep.,* **110,** 50.

Riley, T.R., Leat, P.T., Pankhurst, R.J. & Harris, C., 2001. Origins of large volume rhyolitic volcanism in the Antarctic Peninsulal and Patagonia by crustal melting, *J. Petrol.,* **42**(6), 1043–1065.

Robertson, M.S.D., Wiens, D.A., Shore, P.J., Vera, E. & Dorman, L.M., 2003. Seismicity and tectonics of the South Shetland Islands and Bransfield Strait from a regional broadband seismograph deployment, *J. geophys. Res.,* **108,** doi:10.1029/2003JB002416.

Sandwell, D.T., 1992. Antarctic marine gravity field from high-density satellite altimetry, *Geophys. J. Int.,* **109,** 437–448.

Sandwell, D.T. & Smith, W.H.F., 1997. Marine gravity anomaly from Geosat and ERS 1 satellite altimetry, *J. geophys. Res.,* **102,** 10 039–10 054.

Scheuer, C.K., Gohl, K. & Eagles, G., 2006. Gridded isopach maps from the South Pacific and their use in interpreting the sedimentary history of the West Antarctic continental margin, *Geochem., Geophys. Geosyst.,* **Q11015,** doi:10.1029/2006GC001315.

Schloesser, P., Suess, E., Bayer, R. & Rheim, M., 1988. ^{3}He in the Bransfield waters: indications for local injection from back-arc rifting, *Deep-Sea Res.,* **35,** 1919–1935.

Silant'ev, S.A., Bazulev, B.A., Udintsev, G.B. & Shenke, G.V., 1997. Origin and formation environment of hyperbasite complex of Gibbs Island, South-Shetland Islands, West Antarctica, *Petrology,* **5**(3), 312–325 (in Russian).

Smellie, J.L., 1988. Recent observations on the volcanic history of Deception Island, South Shetland Islands, *Br. Antarct. Surv. Sci. Rep.,* **81,** 83–85.

Smellie, J.L., 1989. Deception Island, in *Tectonics of the Scotia arc, Antarctica,* pp. 146–152, ed. Dalziel, I.W.D., 8th International Geological Congress, Field trip guidebook T180, Washington, DC, Am. Geophys. Un.

Somoza, L., Martínez-Frías, J.L., Smellie, J.L., Rey, J. & Maestro, A., 2004. Evidence for hydrothermal venting and sediment volcanism discharged after recent short-lived volcanic eruptions at Deception Island, Antarctica, *Mar. Geol.,* **203,** 119–140.

Środa, P., Grad, M. & Guterch, A., 1997. Seismic models of the Earth's crustal structure between the South Pacific and the Antarctic Peninsula, in *The Antarctic Region: Geological Evolution and Processes,* pp. 685–689, ed. Ricci, C.A., Terra Antarctica Publication, Siena.

Storey, B.C. & Garrett, S.W., 1985. Crustal growth of the Antarctic Peninsula by accretion, magmatism and extension, *Geol. Magazine,* **122,** 5–14.

Suess, E., Fisk, M. & Kadko, D., 1987. Thermal interaction between back arc volcanism and basin sediments in the Bransfield Strait, Antarctica, *Antarct. J. U.S.,* **22,** 47–49.

Sushchevskaya, N.M. *et al*., 2002. Magmatism of central part of spreading zone of Bransfield Strait (Southern Ocean), *Geochemistry,* **6,** 612–625 (in Russian).

Talwani, M., Worzel, J.L. & Landisman, L., 1959. Rapid gravity computations for two-dimensional bodies with applications to the Mendocino fracture Zone, *J. geophys. Res.,* **64**(1), 49–59.

Tchernychev, M. & Makris, J., 1996. Fast calculations of gravity and magnetic anomalies based on 2-D and 3-D grid approach, in *Proceedings of the SEG 66nd Ann. Internat. Mtd.,* pp. 1136–1138.

Thompson, M.R.A. & Pankhurst, R.J., 1983. Age of Post-Gondwanian calc-alkaline volcanism in the Antarctic Peninsula region, in *Antarctic Earth Science,* pp. 328–333, eds Oliver, R.L., James, P.R. & Jago, J.B., Australian Academy of Science, Canberra.

Udintsev, G.B. & Shenke, G.V., 2004. *Studies of Geodynamics of Western Antarctica,* GEOS, Moscow (in Russian).

Vaughan, A.P.M., Wareham, C.D., Johnson, A.C. & Kelley, S.P., 1998. A Lower Cretaceous, syn-extensional magmatic source for a linear belt of positive magnetic anomalies: the Pacific margin anomaly (PMA), western Palmer Land, Antarctica, *Earth planet. Sci. Lett.,* **158,** 143–155.

Vaughan, A.P.M. & Storey, B.C., 2000. The Eastern Palmer Land shear zone: a new terrane accretion model for the Mesozoic development of the Antarctic Peninsula, *J. Geol. Soc. Lond.,* **157**(6), 1243–1256.

Vaughan, A.P.M., Pankhurst, R.J. & Fanning, C.M., 2002. A Mid-Cretaceous age for the Palmer Land event, Antarctic Peninsula:implications for terrane accretion timing and Gondwana paleolatitudes, *J. Geol. Soc. Lond.,* **159**(2), 113–116.

Vuan, A., Robertson, M.S.D., Wiens, D.A. & Panza, G.F., 2005. Crustal and upper mantle S-wave velocity structure beneath the Bransfield Strait (West Antarctica) from regional surface wave tomography, *Tectonophysics,* **397,** 241–259.

Weaver, S.D., Saunders, A.D. & Tarney, J., 1982. Mesozoic-Cenozoic volcanism in the South Shetland Islands and the Antarctic Peninsula: geochemical nature and plate tectonic significance, in *Antarctic Geoscience,* pp. 263–273, ed. Craddock, C., University of Wisconsin Press, Madison.

Willan, R.C. & Kelley, S.P., 1999. Mafic dike swarms in the South Shetland Islands volcanic arc: unravelling multiepisodic magmatism related to subduction and continental rifting, *J. geophys. Res.,* **104**(B10), 23 051–23 068.

Yegorova, T.P., Stephenson, R.A., Kozlenko, V.G., Starostenko, V.I. & Legostaeva, O.V., 1999. 3-D gravity analysis of the Dnieper-Donets Basin and Donbas Foldbelt, Ukraine, *Tectonophysics,* **313,** 41–58.